AD_____

GRANT NUMBER DAMD17-96-1-6327

TITLE: Comparative Breast Cancer Angiogenesis: Mouse Models

PRINCIPAL INVESTIGATOR: Dr. Robert D. Cardiff

CONTRACTING ORGANIZATION: University of California
Davis, California 95616

REPORT DATE: August 1997

TYPE OF REPORT: Final

PREPARED FOR: Commander
U.S. Army Medical Research and Materiel Command
Fort Detrick, Frederick, Maryland 21702-5012

DISTRIBUTION STATEMENT: Approved for public release;
distribution unlimited

The views, opinions and/or findings contained in this report are those of the author(s) and should not be construed as an official Department of the Army position, policy or decision unless so designated by other documentation.

REPORT DOCUMENTATION PAGE

Form Approved
OMB No. 0704-0188

1. AGENCY USE ONLY *(Leave blank)*	2. REPORT DATE	3. REPORT TYPE AND DATES COVERED
	August 1997	Final (1 Aug 94 - 31 Jul 97)

4. TITLE AND SUBTITLE
Comparative Breast Cancer Angiogenesis: Mouse Models

5. FUNDING NUMBERS
DAMD17-96-1-6327

6. AUTHOR(S)
Dr. Robert D. Cardiff

7. PERFORMING ORGANIZATION NAME(S) AND ADDRESS(ES)
University of California
Davis, California 95616

8. PERFORMING ORGANIZATION REPORT NUMBER

9. SPONSORING/MONITORING AGENCY NAME(S) AND ADDRESS(ES)
Commander
U.S. Army Medical Research and Materiel Command
Fort Detrick, Frederick, Maryland 21702-5012

10. SPONSORING/MONITORING AGENCY REPORT NUMBER

11. SUPPLEMENTARY NOTES

12a. DISTRIBUTION / AVAILABILITY STATEMENT
Approved for public release; distribution unlimited

12b. DISTRIBUTION CODE

13. ABSTRACT *(Maximum 200*

The purpose of this Innovative Idea Grant was to determine whether differences in the microcirculation were critical determinants in the development of metastatic disease in breast cancer. The research was based on a model of mammary cancer in transgenic mice bearing the Polyoma Virus Middle T gene (PyV-MT) promoted by the MuMTV LTR. We previously observed that mice with the wild type gene developed mammary tumors with pulmonary metastases within six weeks of birth (9). However, mice with a PyV-MT construct mutated at positions 315 and 322 (Db-7) developed tumors at a slower rate and rarely developed metastases (8). Transplantable tumor lines were developed by serial transplantation in nude mice (7,8). All transplanted tumors from the wild type PyV-MT (Met-1) developed tumors after 50 or more days (8). Only 10% of the transplanted Db-7 tumors developed metastases (8). The pathologic grade, growth rates, and microcirculation of the metastatic and non-metastatic tumors were compared. The microcirculation, studied using computer assisted imaging and reverse epi-fluorescence, proved to be the only variable that correlated with the metastatic potential of the tumors (8). The microvascular density and the degree of vascular tortuosity (Tortuosity Index) were the only significant variables.

14. SUBJECT TERMS	15. NUMBER OF PAGES
Breast Cancer	32
	16. PRICE CODE

17. SECURITY CLASSIFICATION OF REPORT	18. SECURITY CLASSIFICATION OF THIS PAGE	19. SECURITY CLASSIFICATION OF ABSTRACT	20. LIMITATION OF ABSTRACT
Unclassified	Unclassified	Unclassified	Unlimited

FOREWORD

Opinions, interpretations, conclusions and recommendations are those of the author and are not necessarily endorsed by the U.S. Army.

N/A Where copyrighted material is quoted, permission has been obtained to use such material.

N/A Where material from documents designated for limited distribution is quoted, permission has been obtained to use the material.

✓ Citations of commercial organizations and trade names in this report do not constitute an official Department of Army endorsement or approval of the products or services of these organizations.

✓ In conducting research using animals, the investigator(s) adhered to the "Guide for the Care and Use of Laboratory Animals," prepared by the Committee on Care and Use of Laboratory Animals of the Institute of Laboratory Resources, National Research Council (NIH Publication No. 86-23, Revised 1985).

N/A For the protection of human subjects, the investigator(s) adhered to policies of applicable Federal Law 45 CFR 46.

N/A In conducting research utilizing recombinant DNA technology, the investigator(s) adhered to current guidelines promulgated by the National Institutes of Health.

N/A In the conduct of research utilizing recombinant DNA, the investigator(s) adhered to the NIH Guidelines for Research Involving Recombinant DNA Molecules.

N/A In the conduct of research involving hazardous organisms, the investigator(s) adhered to the CDC-NIH Guide for Biosafety in Microbiological and Biomedical Laboratories.

Robert D Enderlin 8/27/97

PI - Signature Date

TABLE OF CONTENTS
GRANT NUMBER DAMD17-96-1-6327
"Comparative Breast Cancer Angiogenesis" Mouse Models

INTRODUCTION:

The purpose of this Innovative Idea Grant was to determine whether differences in the microcirculation were critical determinants in the development of metastatic disease in breast cancer. The research was based on a model of mammary cancer in transgenic mice bearing the Polyoma Virus Middle T gene (PyV-MT) promoted by the MuMTV LTR. We previously observed that mice with the wild type gene developed mammary tumors with pulmonary metastasis within six weeks of birth (9). However, mice with a PyV-MT construct mutated at positions 315 and 322 (Db-7) developed tumors at a slower rate and rarely developed metastasis (8). Transplantable tumor lines were developed by serial transplantation in nude mice (7,8). All transplanted tumors from the wild type PyV-MT (Met-1) developed tumors after 50 or more days (8). Only 10% of the transplanted Db-7 tumors developed metastasis(8). The pathologic grade, growth rates, and microcirculation of the metastatic and non-metastatic tumors were compared. The microcirculation, studied using computer assisted imaging and reverse epi-fluorescence, proved to be the only variable that correlated with the metastatic potential of the tumors (8). The microvascular density and the degree of vascular tortuosity (Tortuosity Index) were the only significant variables.

Cells from pulmonary metastasis from each of the lines were also serially passaged. The rare metastatic cells from the lungs of Db-7 mice (pD) proved to be highly metastatic when maintained in serial transplant as did the cells from Met-1 metastasis (pMet). The pD cells and the pMet cells also had high microvascular density and Tortuosity Indices.

OUR HYPOTHESIS:

Since current research relates the microvascular density (MVD) in breast cancer to prognosis and since metastatic disease is the most important source of mortality in breast cancer, some investigators have been led to the hypothesis that there is a direct relationship between the MVD and the development of metastatic disease (Weidner N: Tumor angiogenesis: review of current applications in tumor prognostication. *Semin Diagn Pathol* 1993; 10:302-313. Folkman J: Angiogenesis in cancer, vascular, rheumatoid and other disease. *Nature Medicine* 1995; 1:27-31.).

"... new experimental evidence lends itself to a hypothesis that says that the majority of the presenting patterns of metastases may be dictated by the intensity of angiogenesis in their vascular bed." (Folkman J: Angiogenesis in cancer, vascular, rheumatoid and other disease. *Nature Medicine* 1995; 1:27-31.)

What, if any, are the relationships between the metastatic potential of a mammary cancer and the microcirculation? We hypothesized: (a) that increased angiogenesis is necessary but not sufficient for increased metastatic potential and (b) that certain signal transduction pathways are essential for mammary metastases (quite possibly, the PI-3' Kinase pathway). Are (a) angiogenesis and (b) activation of the PI-3' Kinase pathway independent or dependent variables? A fundamental understanding of the metastatic potential of breast cancer requires the ability to discriminate between angiogenesis and critical molecular events in the tumor cells.

The goal of this research program ws to determine whether or not changes in the PyV-MT activated pathways in mammary cancers leading to metastases are also associated with changes in the structure and function of the microcirculation.

The patterns of the microcirculation had never been directly compared in-situ in living animals bearing metastatic or non-metastatic mammary tumors, nor had the angiogenic patterns been directly correlated with the molecular biology of metastatic disease. Therefore, an animal model using mammary cancers with the PyV-MT transgene, was developed to provide the first level separation between angiogenesis and the related molecular events leading to metastasis.

Our transgenic mouse mammary tumor model provides the molecular and biological systems required for the comparative studies of metastatic and non-metastatic tumors and provides well controlled conditions for the objective, quantitative computer-assisted study of angiogenesis.

OUR TECHNICAL OBJECTIVES AND SPECIFIC AIMS:
We proposed to continue our comparative studies in the model system using the following Specific Aims:

1. To compare and contrast the microcirculation of mammary tissues with benign (normal), high and low metastatic potential by completing our in-situ and histological quantitative and qualitative computer-assisted comparisons.

We were funded to complete the first specific aim. The funding was significantly delayed due to the budget crisis in our government. The first aim was completed and is reported below. However, we still are seeking complete funding for the following specific aims which are designed to investigate the molecular basis for our model system. (See submitted and pending grants)

2. To identify, characterize and clone the genes expressed in association with the metastatic process, using differential display.

3. To correlate anomalous microcirculation with the expression of the "metastatic" genes in mammary transplants with benign (normal), high and low metastatic potential using,
   A. *known* gene transcripts or products previously associated with metastases or tumor progression and,
   B. *new* gene transcripts or products developed under Specific Aim #2.

The purpose of this Innovative Idea Grant was to determine whether differences in the microcirculation were critical determinants in the development of metastatic disease in breast cancer. The research was based on a model of mammary cancer in transgenic mice bearing the Polyoma Virus Middle T gene (PyV-MT) promoted by the MuMTV LTR. We previously observed that mice with the wild type gene developed mammary tumors with pulmonary metastases within six weeks of birth (9). However, mice with a PyV-MT construct mutated at positions 315 and 322 (Db-7) developed tumors at a slower rate and rarely developed metastases (8). Transplantable tumor lines were developed by serial transplantation in nude mice (7,8). All transplanted tumors from the wild type PyV-MT (Met-1) developed tumors after 50 or more days (8). Only 10% of the transplanted Db-7 tumors developed metastases (8). The pathologic grade, growth rates, and microcirculation of the metastatic and non-metastatic tumors were compared. The microcirculation, studied using computer assisted imaging and reverse epi-fluorescence, proved to be the only variable that correlated with the metastatic potential of the tumors (8). The microvascular density and the degree of vascular tortuosity (Tortuosity Index) were the only significant variables. Cells from pulmonary metastases from each of the lines were also serially passaged. The rare metastatic cells from the lungs of Db-7 mice (pD) proved to be highly metastatic when maintained in serial transplant as did the cells from Met-1 metastases (pMet). The pD cells and the pMet cells also had high microvascular density and Tortuosity Indices.

BODY:
Metastasis is the major cause of death in breast cancer. The small blood vessels (microcirculation) inside tumors have been correlated with the tendency for human breast cancers to spread (metastasis). However, these studies are retrospective, involving guilt by association. The hypothesis that blood vessels are the critical variables had not been tested in an experimental model. In order to determine the importance of the microcirculation, we developed two closely related transplantable mouse mammary tumors. One tumor (Met-1) metastasizes all of the time (100%). The other tumor (Db-7) rarely metastasizes (>10%) The microcirculation was visualized, studied and filmed inside the tumor using the live animal with a unique illumination technique that allowed detailed, computer-assisted measurements. The small vessels inside the highly metastatic tumors were more complex than those inside the low metastatic tumors. When the low metastatic Db-7 tumor became metastatic, the

microvascular complexity also increased. Other, more traditional measures of the metastatic potential, were studied. The complexity of the microcirculation proved to be the only variable that predicted whether a tumor would metastasize. This model system and these techniques should permit us to study and understand how the metastases can be stopped by altering the microcirculation. The illumination technique may provide an approach for visualizing the microcirculation in human breast cancer.

Details of recent research on Met-1 (metastatic mammary tumor) and Db-7 (low-metastatic mammary tumor) are provided in References #5 and #6 attached to this document. In studying the metastatic potential of Met-1 and Db-7, we have shown that only 10% of the transplanted Db-7 mammary tumors developed metastasis, while 100% of transplanted Met-1 mammary tumors developed metastasis.

In this DOD project, we transplanted Db-7 tumor cells that were harvested from the rare pulmonary metastases (referred to as PD for pulmonary metastasis of Db-7) into donor mice. A transplant line of tumors (PD) were then evaluated for their metastatic potential and microvascular characteristics, using the same methodology described in (6). 14 of 17 (82.4%) transplanted PD tumors developed pulmonary metastasis and in a shorter time period than even the MET-1 tumors. Thus, the cells from the pulmonary metastases from the low metastatic potential Db-7 developed into highly malignant, metastasizing cells.

The microvessel density of the transplanted PD tumors were studied in comparison with Met-1 and Db-7. A significant difference (P=1.73E-08) in the microvessel density existed between PD and Db-7 tumors, with the PD microcirculation showing relatively similar (P=0.6157) microvessel density to Met-1. The microvessel densities of 17 PD tumors, in comparison with Met-1 and Db-7, are tabulated as follows:

See Table-I & Table-II in attachment.

The microcirculation in PD tumors also differed significantly (P=1.2E-04) from Db-7, showing a high degree of vessel tortuosity which was similar to Met-1, with an average Tortuosity Index of 0.47±0.15 in 10 PD tumors studied (Met-1: 0.41±0.1; Db-7: 0.78±0.12).

In summary, changes have occurred in PD -- the microvessel density and vessel tortuosity characteristics of PD differed significantly from Db-7. In addition, PD tumors are highly metastatic (82.4%) as opposed to the low metastatic potential (10%) of Db-7.

CONCLUSIONS:

These experiments show experimentally for the first time that the microvascular circulation is a critical prognostic variable in determining the rate of metastases. They verify the clinical observations in human breast cancer and provide a model system for correlating the changes in microcirculation with the cell and molecular biology and angiogenesis. This model system is very promising since it has proven to be a very effective model for the study of angiogenesis in breast cancer. Furthermore, since the fundamental molecular biology is well understood, this model may provide important molecular clues to the pathways that are critical in angiogenesis and metastasis. Our work has attracted the attention of other investigators and has led directly to additional grant applications.

The research sponsored by the U.S. Army has lead to four abstracts (1-4), two papers (5,6)and one paper submitted (7) . More important these studies have stimulated the submission of three new grants submitted to the U.S. Army (see below) and two others that are in preparation for submission to the National Cancer Institute. The Principle Investigator appreciates the financial support that has led to new avenues of investigation.

REFERENCES:

1. Young, A.T.W.Cheung, W.J. Muller, A. Nodoye, and R.D. Cardiff. Angiogenesis in Malignant Breast Tumors. 86th Annual Meeting of AACR, Toronto 1995

2. Cheung, L.J.T. Young, R.D. Cardiff, A. Nodoye and W.J. Muller. Angiogenesis of a Transplantable Metastatic Mammary Cancer. FASEB Meeting, Atlanta 1995

3. Cheung, P.Y.C. Chen,L.J.T. Young, A. Nodoye, C.Y. Chao, S. Wilttse, W.J. Muller and R.D. Cardiff. Angiogenesis in high- and low-metastatic mammary tumors: an intravital microscopic study. FASEB Meeting, 1996.

4. Bourguignon, Z. Gunja-Smith, N. Iida, H.B. Zhu, L.J.T. Young, and R.D. Cardiff. CD44v3-containing isoform is responsible for vascular endothelial growth factors (VEGF) binding, membrane-cytoskeleton interaction, and matrix metalloproteinases (MMP-9) activation in metastatic breast tumor cells. Am Assoc. Cancer Res. (1996)

5. Cheung, A., P. Chen, L. Young, C. Chao, A. Ndoye, A. Kong and R. Cardiff. Angiogenesis and metastasis in breast tumors. Sixth World Congress for Microcirculation. 23-26 1996.

6. Cheung A.T.W., L.J.T. Young, P. C.Y. Chen, C.Y. Chao, A. Ndoye, P.A. Barry, W.J. Muller, and R.D. Cardiff. Microcirculation and Metastasis in a new mouse mammary tumor model system. Int J. Oncology 11:69-77, 1997

7. L.Y. Bourguignon, Z. Gunja-Smith, N. Iida, H.B. Zhu, L.J.T. Young, and R.D. Cardiff. CD44v3-containing isoform is responsible for vascular endothelial growth factors (VEGF) binding, membrane-cytoskeleton interaction, and matrix metalloproteinases (MMP-9) activation in metastatic breast tumor cells. (Submitted)

8. Guy, C.T., R.D. Cardiff, and W.J. Muller. Induction of Metastatic Mammary Tumors by Expression of Polyomavirus Middle T Oncogene: A Transgenic Mouse Model for Metastatic Disease. Mol.Cell Biol. 12:954-961, 1992.

GRANTS PENDING:

1. Gary Rhodes et. al. - #BC972455
   Immunostimulatory Sequences for Metastatic Breast Cancer Treatment.

2. Earl Sawai et al. - #BC972195
   "Intracellular Signaling Pathways in Metastasis"

3. Peng He et al. - #BC972441
   "Role of Microvessel Permeability in Breast Cancer Metastasis"

GRANT APPLICATIONS IN PREPARATION:

1. R.D. Cardiff, W.J. Muller and . L. Y. Bourguignon

2. A.T.W. Cheung and R.D. Cardiff

3. E. Sawai et al.

PERSONNEL LIST

Personnel receiving pay from this effort:

1. Robert Cardiff, M.D., Ph.D.

2. Anthony Cheung, Ph.D.

3. Debra Marshall

TABLE I

Db-7 (low-metastatic potential)

#	Ref. #	Days Post Tx	100x	200x	Metastasis? (Y or N)
1	2427	14	15	8	N
2	2428	14	18	12	N
3	2431	14	9	6	N
4	2393	15	20	9	N
5	2486	24	12	8	N
6	2396	25	23	8	N
7	2472	32	6	6	N
8	2568	33		9	N
9	2569	33		9	N
10	2421	34	9	4	Y
11	2403	42	20	9	Y
12	2405	42	10	6	N
13	2452	44	4	2	N
14	2453	44	9	6	N
15	2395	45	20	17	N

PD (experimental)

#	Ref. #	Days Post Tx	100x	200x	Metastasis? (Y or N)
1	2643	14			Y
2	2645	18			N
3	2603	15			Y
4	2646	14			Y
5	2624	18			Y
6	2602	9			Y
7	2644	10			Y
8	2606	16			Y
9	2718	26			Y
10	2719	29			Y
11	2720	21			Y
12	2721	31			Y
13	2722	26			Y
14	2723	24			Y
15	2724	17			N
16	2725	21			N
17	2678	29			Y

t-test: Db-7 vs. PD (200x)

	Db-7	PD
Mean	7.8	19.88235
Variance	12.3142857	45.23529
Observations	15	17
t-test (P Value, 2 tail)	1.732E-08	

TABLE II

Db-7 (low-metastatic potential)

#	Ref. #	Days Post Tx	100x	200x	Metastasis? (Y or N)
1	2626	31	32	18	N
2	2627	31	37	21	N
3	2495	37	21	19	N
4	2497	37	25	19	Y
5	2498	37	22	17	Y
6	2397	44	45	43	Y
7	2366	45	45	24	Y
8	2477	45	41	19	N
9	2478	45	37	14	Y
10	2561	46	22	19	N
11	2374	49		26	Y
12	2376	49	44	19	Y
13	2359	50	25	13	Y
14	2345	64		13	Y
15	2432	77	80	51	Y
16	2433	77	22	7	Y
17	2434	77	48	19	Y
18	2435	77	36	34	Y
19	2377	91	56	30	Y
20	2473	91	20	15	Y
21	2474	91	14	10	Y
22	2352		38	18	N

PD (experimental)

#	Ref. #	Days Post Tx	100x	200x	Metastasis? (Y or N)
1	2643			14	Y
2	2645			18	N
3	2603			15	Y
4	2646			14	Y
5	2624			18	Y
6	2602			9	Y
7	2644			10	Y
8	2606			16	Y
9	2718			26	Y
10	2719			29	Y
11	2720			21	Y
12	2721			31	Y
13	2722			26	Y
14	2723			24	Y
15	2724			17	N
16	2719			29	N
17	2720			21	Y

t-test: Db-7 vx. PD (200x)

	Met-1	PD
Mean	21.2727273	19.88235
Variance	107.350649	45.23529
Observations	22	17
t-test (P Value, 2 tail)	0.61570706	

Sixth World Congress for Microcirculation

Munich, Germany
25-30 August 1996

Angiogenesis and metastasis in breast tumors

A. CHEUNG, P. CHEN *, L. YOUNG, C. CHAO **, A. NDOYE, A. KONG and R. CARDIFF

Department of Medical Pathology
University of California, Davis School of Medicine, Davis, CA (USA)
* *Department of Bioengineering*
University of California, San Diego, La Jolla, CA (USA)
** *Department of Pathology*
Fourth Military Medical University, Xian, People's Republic of China

SUMMARY

High-metastatic potential [Met-1] and low-metastatic potential [Db-7] breast tumors have been established as an experimental platform for angiogenesis (intratumoral microvessel density [MVD]), microcirculation and metastasis research. With the utilization of *computer-assisted intravital microscopy and histopathology/immuno-histochemistry procedures*, it has been revealed that angiogenesis is a significant variable in the metastatic process. The tumor microcirculation of Met-1 is complex and heterogeneous, and the internal microvessels exhibit tortuous paths. Microvessel tortuosity (measured as Tortuosity Index [TI]) is a unique intratumoral feature. The TIs (Met-1: 0.41±0.01/Db-7: 0.78±0.02; P<0.0001) are highly significant measurements and TI for Met-1 correlates with a high MVD (20.2±9.7 microvessels/200x field & 32.6±12.9 microvessels/100x field) and a high metastatic rate (12/14) in the Met-1 high-metastatic potential breast tumors, using the low MVD (7.6±3.7 microvessels/200x field & 13.5±6.2 microvessels/100x field) and low metastatic rate (2/13) of Db-7 as low-metastatic potential control.

INTRODUCTION

Angiogenesis and microcirculation play a vital role in the development and growth of solid tumors (1,2). Since metastatic disease is the major source of mortality in human breast tumor patients, one is led to assume that there is a direct relationship between angiogenesis and metastasis. Indeed, current concepts, including the seminal works of Weidner, Folkman, et al, suggest a strong correlation between angiogenesis and prognosis in human breast tumor patients (3,4), although there has been no direct evidence to link angiogenesis with metastasis.

Since it is neither ethical nor feasible to work directly with human patients, the development of high-metastatic and low-metastatic potential tumor models and new *in vivo* technologies to objectively study angiogenesis and metastasis is warranted.

Two transplantable breast tumor lines (Met-1/high metastatic potential and Db-7/low-metastatic potential), from Polyoma Virus Middle-T [PyV-MT] transgenic breast tumors, have been established in the nude mice as an experimental platform for this study. We have further developed new technologies in computer-assisted intravital microscopy and histopathology/immuno-histochemistry to videotape the microcirculation inside the solid tumor(s) and to study intratumoral characteristics, including microcirculation organization, microvessel tortuosity and microvessel density [MVD]. The results are correlated directly with metastasis in the same animals studied. We hypothesize that complex microcirculation organization and microvessel tortuosity are unique intratumoral features in metastatic tumors. Our goal is to confirm the exclusive presence of these microvascular characteristics in Met-1, their absence in Db-7, and that they can be used to correlate and explain the high MVD identified by Weidner for human breast tumor prognosis. The significance of this project is underscored by the ability to evaluate microvessel tortuosity and MVD (angiogenesis) in tumor tissues and to link this data with pulmonary metastasis in the same animals.

MATERIALS AND METHODS

Animal Model. Female athymic (BALB/c nu/nu) nude mice, 5-6 weeks old, were used. Met-1 and Db-7 breast tumors were transplanted into the fat pads (*orthotopic* site) of nude mice to serve as model for microcirculation and MVD studies.

Met-1 (high-metastatic potential) breast tumor line. This tumor line was derived from the PyV-MT transgenic colony at Dr. Muller's Institute for Molecular Biology and Technology at McMaster University, Hamilton, Ontario, Canada. Breast tumor cells containing the PyV-MT transgene were used to initiate this transplantable Met-1 line in nude mice. The resulting Met-1 high-metastatic potential breast tumor line has now passed transplantation generation #15 in this laboratory.

Db-7 (low-metastatic potential) breast tumor line. This tumor line was also derived from the PyV-MT transgenic colony at McMaster University. This transplantable line resulted from a double base mutation at positions 315 and 322 and has now passed transplantation generation #15. Because of its low-metastatic potential, it was utilized as control for Met-1 in microvessel tortuosity, MVD (angiogenesis) and metastasis studies.

Establishment of the Met-1 and Db-7 animal models. Pieces of Met-1 or Db-7 tumors were transplanted into the 4th inguinal mammary fat pads of recipient nude mice to establish the tumor models for research use. Each host nude mouse was anaesthesized with IP sodium pentobarbital (60mg/Kg). A 1.5-cm midline incision was made on the ventral wall, midway between the #4 nipples of the inguinal mammary glands. The incision was further extended to reach the #5 nipples. The skin flaps were retracted to expose the #4 fat pads underneath the nipples. A 1-mm^3 piece of the tumor (Met-1 or Db-7) was transplanted with a 45° angled jeweller's forcep into an intact fat pad (*orthotopic* site) and the skin flaps were closed with 9-mm wound clips.

Computer-assisted intravital microscopy (*Intravital microscope system on-line with data quantitation/imaging system*).

Intravital microscope system. An intravital microscope system was built for this study. Its design was based on, and adapted substantially from, a previous prototype (5). With the tumors exposed by releasing the wound clips, the intratumoral microcirculation of Met-1 and Db-7 were videotaped under intravital conditions. Upon completion of microscopy, the animals were sacrificed and the primary tumors were processed, sectioned and stained (H&E and α-actin) for MVD evaluation.

Data quantitation/imaging system. Data quantitation was conducted by computer-assisted image analysis with in-house developed software. Videotape sequences of the microcirculation of Met-1 and Db-7 were selected, coded and blindly quantitated for morphometric and microvascular characteristics.

Metastasis Evaluation. The metastatic capability of Met-1 and Db-7 was evaluated by histopathology. The lungs, liver, spleen, brain, kidneys and lymph nodes of all the animals were collected and studied grossly. The organs/tissues were subsequently processed, sectioned (4-μm), stained (H&E) and scored for metastasis by a pathologist.

Microvessel density [MVD] evaluation. The primary tumor (Met-1 or Db-7) was processed for histopathology study. Four μm sections were cut and immuno-stained for α-actin. Anti-α-actin antibodies were applied to the 4-μm sections at 1:200 dilution and counter-stained using standard immunoperoxidase staining procedure. Each stained slide was scanned and examined under light microscopy at 100x to identify MVD "hot-spots", stained cross-sections of microvessel cluster(s) or angiogenic microvessels. Upon identification, the number of stained cross-sections and/or microvessels was counted. The magnification was switched to 200x and the number of "hot-spots" was again counted. The MVD for each tumor was scored as the number of microvessels per field (200x and 100x) for each tumor.

Vessel tortuosity evaluation. Videotapes were viewed and video sequences containing well-resolved microvessels were selected and coded for subsequent analysis. One frame of the microcirculation from each selected sequence was grabbed and digitized with the assistance of an on-line imaging board (frame-grabber). Two arbitrary points were marked on the on-screen image of the microvessel being evaluated. Via computer-assisted image analysis, the direct (shortest) length between the two points was measured. The actual length of the meandering microvessel from one point to the other was also measured. The Tortuosity Index [TI], an indicator of the tortuosity (curvature) of the microvessel, was calculated as the shortest length between two points in the microvessel divided by the actual length of the meandering microvessel between the same two points.

Statistics. Changes in variables were analyzed using ANOVA and Student's T-test whenever appropriate. A 0.05 significance level was used.

RESULTS

Met-1 and Db-7 transplantations into fat pads of nude mice were successful in all cases. Angiogenesis started 2-3 days post-transplantation in both Met-1 and Db-7 breast tumors. Angiogenesis and microcirculation development progressed rapidly in a similar manner in both tumor lines for 6-7 days. The external (surface) microcirculation of Met-1 and Db-7 was similar throughout this study (2-23 days). However, significant differences in the intratumoral (internal) microcirculation between Met-1 and Db-7 started to appear 6-7 days post-transplantation. Angiogenic development occurred more rapidly in Met-1 and the intratumoral microcirculation became complex and heterogeneous. In addition, the intratumoral microvessels in Met-1 became extremely tortuous. The Db-7 microcirculation, though also heterogeneous, was less dense and poorly organized. In addition, Db-7 internal microvessels were relatively non-tortuous in their paths.

Metastasis. The metastatic rate for Met-1 (12/14; 85.8%) differed significantly ($P<0.0001$) from Db-7 (2/13; 15.4%). In all the animals investigated, metastatic foci were only found in the lungs.

Intratumoral microvessel density [MVD] (angiogenesis). Intratumoral angiogenic microvessels were identified by immuno-staining. Microvessel distribution inside Met-1 and Db-7 were heterogeneous and MVD "hot-spots" (clusters) were present in some areas but absent in other areas. However, as a rule, whenever "hot-spots" were located and scored, the MVD was significantly higher ($P<0.0001$) in Met-1 (20.2±9.7 microvessels/200x field; 32.6±12.9 microvessels/100x field) than in Db-7 (7.6±3.7 microvessels/200x field; 13.5±6.2 microvessels/100x field).

Tortuosity. Tortuosity for all intratumoral microvessels was expressed as a Tortuosity Index [TI]. The microvessels in Met-1 were extremely tortuous (TI=0.41±0.01) and differed significantly ($P<0.0001$) from the relatively non-tortuous microvessels in Db-7 (TI=0.78±0.02).

CONCLUSIONS

This project has demonstrated that angiogenesis is indeed a significant variable in the metastatic process. We have documented that microvessel tortuosity is a unique intratumoral feature and that the Tortuosity Index for a tumor (e.g. Met-1) is highly significant and correlates with intratumoral MVD (angiogenesis) and metastasis in the same animal(s). The microvessel tortuosity in Met-1 can also explain the high MVD in metastatic solid tumors as the abundance of "hot-spots" may represent the result of histological sectioning across highly tortuous (instead of straight) microvessels. This study quantitatively validates the utilization of MVD as a prognostic marker for breast tumor metastasis in nude mice and the results can be extrapolated for human interpretation.

REFERENCES

(1) Gullino PM and Grantham FH. The vascular space of growing tumors. *Cancer Res* 24:1727-1732, 1964.
(2) Jain RK. Determinants of tumor blood flow. *Cancer Res* 48:2641-2658, 1988.
(3) Weidner N. Tumor angiogenesis: Review of current applications in tumor prognostication. *Semin Diagn Pathol* 10:302-313, 1993.
(4) Folkman J. Angiogenesis and breast cancer. *J Clin Oncol* 12:441-443, 1994.
(5) Cheung ATW, Bry WI, Cox KL and Ahlfors CE. Reversal of microangiopathy in long-term diabetes after successful simultaneous pancreas-kidney transplants. *Transpl Proc* 25:1310-1313, 1993.

Microcirculation and metastasis in a new mouse mammary tumor model system

ANTHONY T.W. CHEUNG[1], LAWRENCE J.T. YOUNG[1], PETER C.Y. CHEN[2], CHIEN Y. CHAO[3], ASSANE NDOYE[1], PETER A. BARRY[1], WILLIAM J. MULLER[4] and ROBERT D. CARDIFF[1]

[1]Department of Medical Pathology, School of Medicine, University of California, Davis, CA 95616; [2]Institute for Biomedical Engineering, University of California, San Diego, La Jolla, CA 92093, USA; [3]Department of Pathology, 2nd Teaching Hospital, 4th Military Medical University, Xian 710038, P.R. China; [4]Institute for Molecular Biology and Technology, McMaster University, 1280 Main St. West, Hamilton, Ontario L8S 4K1, Canada

Contributed by R.D. Cardiff, April 18, 1997

Abstract. Two new metastatic mouse mammary tumor transplant lines have been established in nude mice. The Met-1 line, with the polyoma virus middle T (PyV-MT) transgene, metastasized with 100% efficiency. The Db-7 line, expressing a PyV-MT transgene mutated at positions 315 and 322, metastasized with 8.8% efficiency. Histology and computer-assisted intravital microscopy demonstrated that internal microcirculation in Met-1 was more complex than Db-7; Met-1 exhibited higher microvessel density and tortuosity ($P<0.0001$). These indices of microvascular complexity correlated with the higher Met-1 metastatic rate ($P<0.0001$). These two transplantable lines will be useful for investigating the complex relationship between angiogenesis and metastasis.

Introduction

Angiogenesis and microcirculation play a vital role in the development, growth and metastasis of tumors (1-4). The pathophysiology of tumor angiogenesis was first delineated experimentally by Coman and Scheldon (2), Gullino and Grantham (3). The field of tumor angiogenesis was later expanded by a number of investigators who showed that transplanted tumors could not grow without angiogenic vessels and subsequent established microcirculation (4-10). Neovascularization was essential for supplying nutrients and oxygen, and the removal of waste products, during tumor growth and development. The literature on microvascular morphology, angiogenesis and the tumor microcirculation has been extensively reviewed (1,6-18). The discovery of angiogenic and anti-angiogenic factors has raised intriguing and far-reaching therapeutic possibilities (19-21).

Correspondence to: Dr Robert D. Cardiff, Department of Medical Pathology, School of Medicine, University of California, Davis, CA 95616, USA

Key words: angiogenesis, microcirculation, microvessel density, metastasis, mammary tumors, tortuosity index

Successful treatment of human breast cancer depends on limiting metastatic dissemination of the primary tumor. The development of appropriate treatment protocols could be assisted by the development of relevant animal tumor models to study the relationship between tumor growth, metastasis, and other factors affecting tumor progression, such as angiogenesis and tumor microcirculation. However, few animal models of mammary tumor metastasis are available which lend themselves to the direct and simultaneous study of the critical factors.

The concepts of tumor angiogenesis and microcirculation have been primarily based on tumors transplanted into readily observable ectopic sites, including subcutaneous tissues, eye chamber, rodent dorsal skin-window, rodent transplant chamber and rodent cranial-window (3-5,22-24). These studies have been limited by focusing exclusively on the surface (external) microcirculation of tumors transplanted at ectopic sites and by short observation times of tumor growth and angiogenesis. Further, most human breast cancers do not metastasize when transplanted into animal models. Even transplants from metastatic foci rarely metastasize after transplantation (25-30). Thus, the nature of the microcirculation inside the tumors during the time that metastasis is actually occurring has not been adequately studied.

Recent histological studies showing high intratumoral microvessel density (MVD) (microvessel hot spots) inside primary breast cancers have highlighted the need for new approaches to the study of the microcirculation inside solid breast tumors (13-16). These studies have noted an association between high MVD inside the tumor and poor prognosis in human breast cancer (13-16). However, a direct relationship between MVD and metastasis has not been experimentally established.

To address the limitations inherent in the previous studies, we developed an effective computer assisted intravital microscope (CAIM) to study the *in vivo* relationships between angiogenesis, internal microcirculation, MVD and metastasis in a new mammary tumor model of metastasis. First, highly metastatic (Met-1) and low metastatic (Db-7) mammary tumor lines, from polyoma virus middle T (PyV-MT) transgenic mammary tumors, were established by orthotopic trans-

plantation into the mammary fat pad. The Met-1 line was developed from tumors arising in transgenic mice, and the Db-7 line was developed from tumors in transgenic mice expressing a PyV-MT transgene mutated at sites 315 and 322 (31-33). Secondly, a CAIM using reverse epi-fluorescence illumination was developed to quantitate the intratumoral microcirculation. The CAIM documented the differences between the microcirculation of Met-1 and Db-7. The degree of tortuosity and high MVD of the internal microcirculation proved to be indices that correlated with the extremely high metastatic rate (100%) in Met-1 and differed significantly from the low tortuosity, low MVD and low metastatic rate (8.8%) in Db-7.

Materials and methods

Materials: animals. Female athymic nude mice (BALB/c nu/nu), 5-6 weeks old, were used. They were purchased from Simonsen (Gilroy, CA), Charles River (Wilmington, MA), B&K Universal (Freemont, CA) and Taconic (Germantown, NY) Laboratories. The transplanted Met-1 and Db-7 tumors developed well in all nude mice used, regardless of vendor or origin. All experimental nude mice were housed in a laminar flow cabinet, given sterile water and fed *ab libitum*.

Metastatic polyoma virus middle T transgenic (Met-1) mammary tumor line. Mammary tumor cells containing the PyV-MT transgene under the transcriptional control of the MMTV LTR promoter were used to initiate transplantable metastatic Met-1 lines in nude mice (31). The PyV-MT transgenic mammary tumor cells were derived from mammary tumors from the transgenic FVB colony at the Institute for Molecular Biology and Biotechnology, McMaster University, Hamilton, Ontario, Canada. Mammary tumors were collagenase/dispase (Worthington, Freehold, NJ) processed, and a bolus inoculum of $5x10^5$ cells per 100 µl were transplanted subcutaneously via syringe and a 25-gauge needle into the thoracic region of recipient nude mice.

The resulting metastatic PyV-MT transgenic mammary tumor line was maintained by serial transplantation of 1-2 mm^3 tumor segments, and is now in transplantation generation No. 26. Tumor tissues for experimental use were transplanted into the intact inguinal fat pads (orthotopic site) or subcutaneously (ectopic site) of female nude mice for comparison. Sodium pentobarbital (Nembutal, Abbott Laboratories) given intraperitoneal (IP) at 60 mg/kg was used as anesthesia during tumor transplantation and removal. Met-1 tumors were used to develop a cell culture line which is currently in passage No. 25. Growth size of the tumors over time was determined by daily caliper measurements.

Low-metastatic polyoma virus middle T transgenic (Db-7) mammary tumor line. The low metastatic Db-7 mammary tumor line was developed in the same manner as the Met-1 line. The Db-7 tumor line arose in FVB mice with the PyV-MT transgene containing a double base, site-directed point mutations at positions 1194 and 1215, resulting in A-T transversions (substituting a phenylalanine for tyrosine at each residue), and corresponding to amino acids 315 and 322 respectively. The Db-7 line was maintained as described for the Met-1 line, and has now passed transplantation generation No. 19. Transplantation of Db-7 tumors in nude mice was conducted in the same manner as in Met-1. A Db-7 cell culture line was also developed and is currently in passage No. 44.

Establishment of the mammary tumors in animals. For tumor establishment, pieces of Met-1 or Db-7 tumors (or tumor tissues) were transplanted into the 4th inguinal mammary fat pads of the recipient nude mice. Each recipient mouse was anesthetized with IP sodium pentobarbital (60 mg/kg). A 1.5-cm mid-line incision was made on the ventral wall, midway between the No. 4 nipples of the inguinal mammary glands. The incision was further extended to reach the No. 5 nipples. The skin flaps were retracted to expose the underlying No. 4 fat pads. A 1-mm^3 piece of the tumor or tissue was transplanted with a pair of 45° angled jeweler's forceps into an intact fat pad (orthotopic site) for study. For ectopic site comparison, transplantation of the 1-mm^3 piece of the tumor or tissue was conducted at the exposed subcutaneous tissue away from the fat pads. The skin flaps were closed with 9-mm wound clips after transplantation.

Polymerase chain reaction/PyV-MT transgene confirmation. The presence of the PyV-MT transgene in the Met-1 and Db-7 tumors was determined by polymerase chain reaction (PCR) of cells obtained from the original tumor tissues, the resulting tumors, and cells from every other transplant generation. The PCR primers were (5'-ATA GAG TTC TGA GCA GAG-3') corresponding to positions 193-210 of PyV, and (5'-CGT TGT ATC TCT CGA GTT-3') corresponding to positions 592-575 of PyV (Genbank No. J02289).

Equipment: intravital microscopy. The intravital microscope system was specifically designed and built for this project. Its design was based on, and modified substantially from, a previous prototype developed earlier in this laboratory for the evaluation of diabetic nailfold microangiopathy (34,35). Olympus optical elements (Scientific Instrument Company, Sunnyvale, CA) were used in the fabrication of the intravital microscope system. The light source consisted of a DC mercury burner, and the intravital microscope was equipped with epi-brightfield and epi-fluorescence illumination capabilities. The infinity-corrected optical elements were assembled in a metallurgical microscope body which was anchored to a heavy granite base by a steel post attachment. A FOR-A model No. VTG-33 video-timer was installed for on-screen digital time display. Tumor microcirculation was videotaped with a high-resolution COHU model No. 6415-3000 CCD video-camera. The intravital procedure was adapted from a reverse epi-fluorescence illumination technique which was originally developed in this laboratory for the *in vivo* investigation of choledochoduodenal junction motility and gallstone formation in the guinea pig (36,37).

Data quantitation. Data quantitation was conducted by computer-assisted image analysis procedures with the application of VASCAN, an in-house developed imaging software (37). The intravital microscope system was put on line, via the video-recorder, with the computer-assisted imaging system. Objective quantitation could be conducted

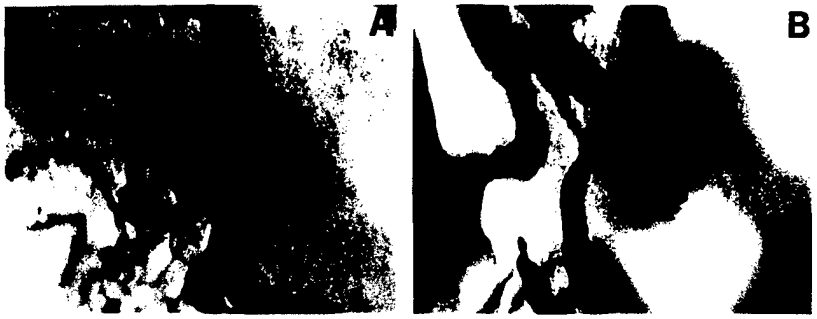

Figure 2. Two selected views of the internal microcirculation of Db-7 videotaped under intravital microscopy (magnification: x150). A, A view of the internal microcirculation in Db-7 13-days post-transplantation. Note the difference in organization pattern compared with Met-1 (Fig. 1D and F). B, A view of the internal microcirculation in Db-7 23-days post-transplantation. Note the relatively straight paths and the paucity of vasculature.

spaces inside the tumor mass. As a result, the intratumoral microvessels appeared as crisp black lines or solid black tubes with a bright white/fluorescent background when viewed under epi-fluorescence illumination (Figs. 1 and 2). The microcirculation of both highly metastatic and low metastatic mammary tumors were studied with this intravital protocol. It should be noted, however, that special emphasis was placed on studying the internal microcirculation at a depth of 250-350 μm inside the solid tumor mass.

The tumors to be studied were exposed via a mid-line incision and retraction of the skin-fold. A still photograph (via macro-photography) and a short videotape sequence of the tumor surface were taken to show the external tumor microcirculation (34-37). To study the internal tumor microcirculation, focus of the CCD video-camera was aimed at the inside of the tumor mass, 250-350 μm away from the surface, via intravital microscopy under reverse epi-fluorescence illumination. The internal tumor vessels literally appeared as crisp black lines or tubes inside the bright fluorescent/white tumor mass (Figs. 1 and 2). Videotapes were made for subsequent analysis and computer-assisted data quantitation.

Data quantitation/image analysis. Videotapes on intratumoral (internal) vessels and the microvascular network were coded and studied blindly. Each videotape was viewed in its entirety on the monitor screen via video playback. Short video sequences were chosen for quality of the image and microvascular features. Each chosen sequence was coded for subsequent blinded computer-assisted data quantitation. With the utilization of the imaging-board and the application of the VASCAN imaging software, a video frame from each video sequence was grabbed and digitized (38). Quantitative measurements of the microvascular characteristics, including vessel morphometry and distribution density (utilizing a scan and gray level trace algorithm) and perfusion characteristics of the microvessels (utilizing a 120-μm expansion algorithm), were generated and printed out for interpretation (38).

Microvascular pattern/tortuosity. The tortuosity of the internal and external microcirculation was studied via analysis of the videotapes. The internal microvessels in Met-1 were analyzed for tortuosity and compared with the external microvessels in the same tumor. The internal microvessels in Met-1 were also compared with the internal microvessels in Db-7.

Video sequences on the internal microcirculation of Met-1 and Db-7 and external microcirculation of Met-1 were selected and coded. Each coded sequence was viewed and one frame with good resolution was chosen, grabbed and digitized. Two arbitrary points were put on each vessel in the frame to be studied. By computer-assisted imaging, the direct (shortest) length between the two points was measured. Then, the actual meandering length of the vessel from one point to the other was also measured. The tortuosity index, which was an indicator for the meandering path of each vessel, was computed as the shortest (straight-line) length between the two points in the vessel divided by the actual length of the meandering vessel between the same two points (shortest distance/actual distance). The results were used for comparison and subsequent statistical analysis.

Microvessel density (MVD). Four μm sections of the primary tumors were cut and immunostained for α-actin. Anti-α-actin antibodies (Boehringer Mannheim Biotechnology, Indianapolis) were applied to the 4-μm sections at 1:200 dilution and counter-stained using standard immunochemistry staining procedures. The stained slides were scanned and examined under light microscopy at 100x to identify MVD hot spots which were cross-sections of immunostained microvessel clusters or segments, depending on the plane of sectioning. These MVD hot spots were counted and expressed as No. microvessels per 100x field. The magnification was switched to 200x and the hot spots were again scored as No. microvessels per 200x field. All the slides were coded for counting. Each slide was scored blindly and separately by three individuals, and the results were averaged; variations were adjudicated by these three individuals. The averaged scores were tabulated for subsequent statistical analysis. A threshold value was not assigned to indicate a high or low MVD score. Instead, the MVD values for the highly metastatic and low metastatic tumors were tabulated (Table II) for direct comparison and subsequent computation for statistical significance.

Metastasis. The metastatic capability of Met-1 and Db-7 mammary tumors was evaluated by histopathology. The lungs, liver, spleen, brain, kidneys and lymph nodes of all the animals were collected and studied grossly. The collected tissues/organs were subsequently processed, sectioned (4-μm),

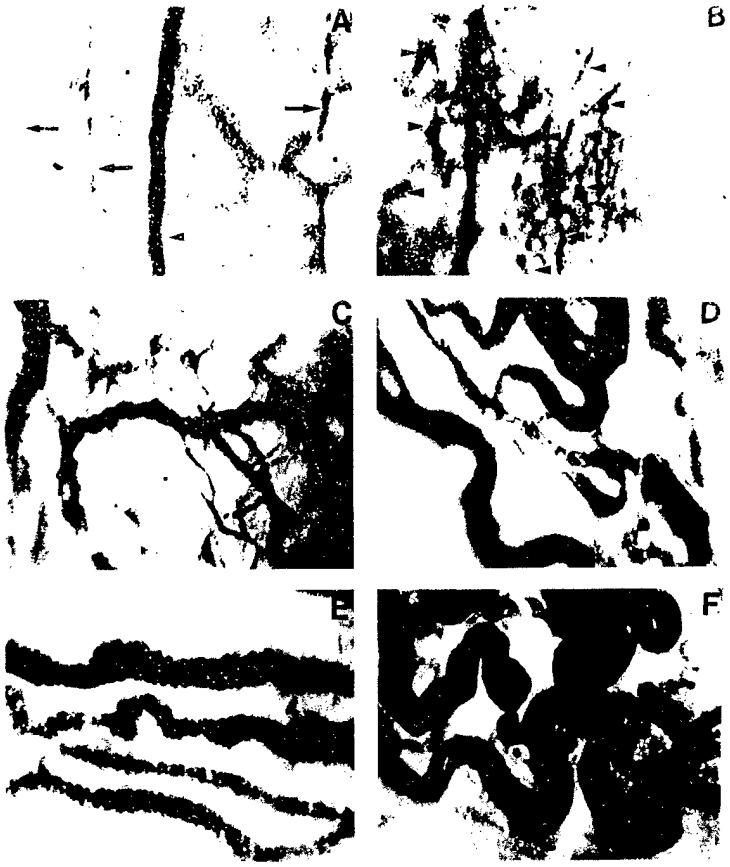

Figure 1. Six selected views of the pre- and post-transplantation tumor microcirculation of Met-1 videotaped under intravital microscopy (magnification: x150). A, A view of a pre-transplantation control showing the normal subcutaneous microcirculation at the neighboring site of the fat pad into which Met-1 was to be transplanted. This figure represents a view of the normal subcutaneous microcirculation, with the presence of three (3) parallel post-capillary venules (arrows), and with one (1) venule draining into a larger vein (marker). B, An internal view of a transplanted Met-1 tumor mass 4-days post-transplantation. The angiogenic vessels appear as black lines (neovessels) or fragmented black lines (sprouts to be joined to form a neovessel). The sprouts are indicated by markers. C, An internal view of a transplanted Met-1 tumor 10-days post-transplantation, showing a complex network of microvessels with arterio-venous anastomosis. D, A view of the internal microcirculation of Met-1 13-days post-transplantation, showing complex microvascular organization with tortuous vessels. E, A view of the external microcirculation on a Met-1 tumor 23-days post-transplantation, showing the straight external vessels. F, A view of the internal microcirculation inside the Met-1 tumor mass (in the same tumor in E) showing the complex and tortuous internal vessels

on real time or via videotape. The computer system utilized a PC-based platform and was installed with a data translation model No. DT2803 imaging board.

The computer-assisted quantitation provided morphometric and functional analysis of the tumor microcirculation as the software was written to objectively measure 25 different microvascular parameters. In this study, however, measurements were limited to quantitating morphometric characteristics, microvessel distribution and perfusion characteristics of the microcirculation only. In view of the variation of microvessel density inside any solid tumor mass and the heterogeneity of the intratumoral microvasculature, the ability to objectively measure the microcirculation uniquely underscored the significance of this study.

Methods: intravital procedure. The tumor microcirculation was videotaped under specialized intravital microscopy (34-37) and the surface/external as well as intratumoral/internal (250-350 μm deep) microcirculation of the solid mammary tumors (both Met-1 and Db-7) could be easily videotaped (Figs. 1 and 2). In this laboratory, we have four available intravital microscopy protocols to videotape tumor microcirculation: i) Using the dorsal skin-window technique with transmitted illumination on an implanted tumor inside the window-chamber, ii) Using lateral (quartz rod) illumination on the surface of a transplanted tumor, iii) Using epi-fluorescence illumination with injected FITC-dextran (fluorescent/white microvessels with a dark gray background) inside a transplanted tumor, and iv) Using epi-fluorescence illumination with injected sodium fluorescein (black microvessels with a fluorescent/white background) inside a transplanted tumor. We have experimented with all four protocols, and had attained the best resolution with optimal depth penetration (250-350 μm inside the tumor mass) with protocol (iv), utilizing intravital microscopy coupled with sodium fluorescein induced reverse epi-illumination. As a small molecular-sized fluorescence dye, injected sodium fluorescein leaked readily and profusely into extravascular

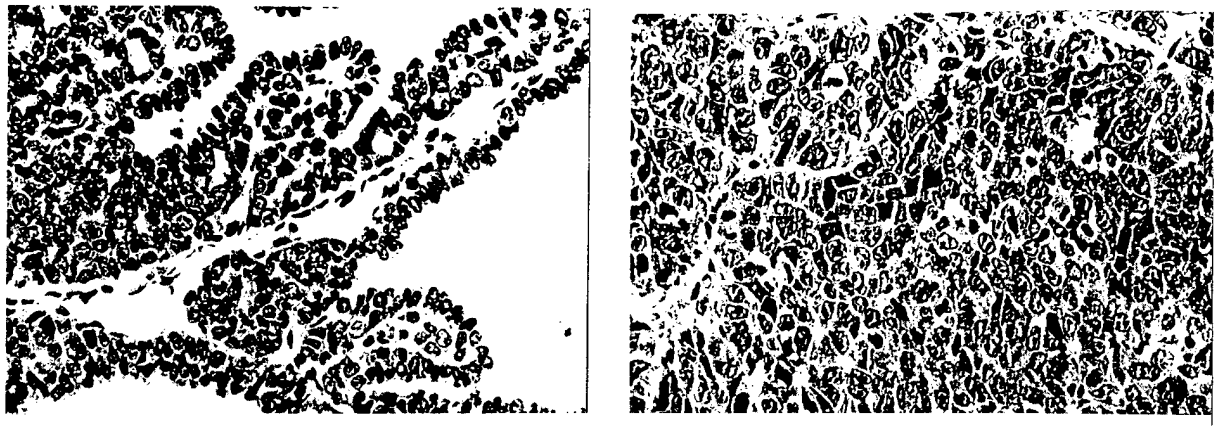

Figure 3. Histological sections of Met-1 and Db-7 mammary tumors. A, H&E stained section showing a typical Met-1 transplanted mammary tumor. Note the papillary growth pattern with small glands within the epithelium. The luminal space is filled with acellular, pink fluid, and apical blebs appear above the surface. Magnification is x400. B, H&E section showing a typical Db-7 transplanted mammary tumor. Note the presence of pleomorphic cells with a solid growth pattern, the absence of glandular differentiation, and the large number of mitotic figures (11 in this field). Magnification is x400.

Table I. Comparison of developmental characteristics between Met-1 and Db-7 mammary tumors.

Characteristics	Met-1	Db-7
Histological pattern	Glandular	Lobular
Pleomorphism	+	+++
Necrosis	+	++
Mitotic figures	2.8/hpf	10/hpf
Metastasis	High - 100%	Low - 8.8%
Pulmonary metastasis	Embolism, invasive	Embolism
SBR score	4.7	6.1

Table II. Comparison of intratumoral microvascular characteristics between Met-1 and Db-7 mammary tumors.

Microvascular characteristics	Met-1	Db-7
Tortuosity index (internal vessels)	0.41±0.1	0.78±0.12
Microvessel density (MVD) per 100x field	32.6±12.9	13.5±6.2
Microvessel density (MVD) per 200x field	20.2±9.7	7.6±3.8
Venule diameter (μm)- 23 days post-transplant	84.6±7.8	68.1±5.4
Percent adequately perfused area[a]	34.8±8.3[c]	18.9±6.5[c]
Percent marginally/ inadequately perfused area[a]	44.9±19.8[d]	69.4±10.9[d]
Microvessel surface area/region[b]	17.4±5.5	5.3±1.7
Microvessel volume/region[b]	36.7±7.8	9.8±3.2
Microvessel length/region[b]	55.6±10.3	16.2±4.5

[a]Area studied, 6.25 mm^2; [b]Region studied, 8.53 mm^2; [c]Subcutaneous tissue control range, 58-76%; [d]Subcutaneous tissue control range, 2-11%.

stained (H&E) and studied microscopically for metastasis by a pathologist.

Statistics. Changes in variables were analyzed using ANOVA or Student's t-test. A 0.05 significance level was used. P-values lower than 0.0001 (e.g. $P=4.8\times10^{-17}$ for metastatic incidence, $P=2\times10^{-10}$ for tortuosity index and $P=9\times10^{-5}$ for MVD) were all reported as $P<0.0001$ for simplicity.

Results

Met-1 metastatic tumor. The Met-1 metastatic tumor line formed moderately well differentiated to poorly differentiated papillary adenocarcinomas when transplanted into either orthotopic (fat pad) and ectopic (subcutaneous) sites (Fig. 3A). Sporadic necrotic and hemorrhagic areas were sometimes present inside the tumors. The histological grade, based on the Scarff-Bloom-Richardson (SBR) system (39), was 4.7 for the Met-1 tumors (Table I). The histopathological pattern and SBR grade were maintained throughout all transplant generations studied. Mitotic cells could be seen in histological sections (2.8/hpf).

Transplanted tumors in either orthotopic and ectopic sites were palpable 4-days post-transplantation. The growth rate of the Met-1 tumors at the orthotopic site, as measured by increases in tumor size, was twice that of ectopic site (data not shown).

Db-7 low-metastatic tumor. The transplantable Db-7 tumor line formed poorly differentiated carcinomas in either orthotopic and ectopic sites (Fig. 3B). Similar to Met-1 tumors, the growth rate of the Db-7 tumors at the orthotopic site was

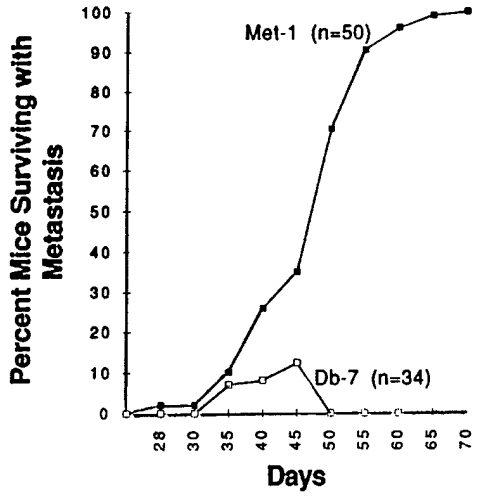

Figure 4. Comparison of the rate of metastasis (percent metastasis over time) from Met-1 and Db-7 mammary tumors. Each data point was calculated from the number of animals found with pulmonary metastasis divided by the total number of animals sacrificed for metastasis during a given time period multiplied by 100.

twice that of ectopic site. However, Db-7 exhibited a higher growth rate than Met-1 in both orthotopic and ectopic sites (e.g. growth rate for Db-7 from 5th day through 14th day was twice Met-1 at orthotopic site). More necrotic and hemorrhagic areas were seen inside the Db-7 tumors, and more mitotic cells were present (10/hpf).

Metastasis. Nude mice with either Met-1 or Db-7 orthotopic transplants were terminated between 23 and 91 days after tumor transplantation, and organs and tissues were harvested to evaluate metastasis.

Metastatic foci, found only in the lungs, were either unifocal or multifocal clusters. Met-1 gave rise to early (28 days) detectable pulmonary metastasis. At 50 days post-transplantation, the metastatic incidence for Met-1 was 70%. The metastatic incidence rose significantly to 90% by 54 days and 100% after 65 days. In contrast, only three of 34 animals (8.8%; $P<0.0001$) transplanted with the Db-7 tumor line developed pulmonary metastasis by the 42nd day. In a follow-up evaluation involving nine nude mice, none kept over 42 days developed metastases (Fig. 4).

The presence of the PyV-MT transgene was used to verify the origin of the pulmonary foci. PCR analysis confirmed the presence of the PyV-MT wide-type and double-mutant transgenes in the DNA of the Met-1 and Db-7 tumors, respectively (data not shown).

Angiogenesis and tumor microcirculation. Control microcirculation: the normal microcirculation was represented by the pre-transplant microvascular network at the transplant sites. Fig. 1A showed a typical view of small parallel (non-tortuous) post-capillary venules merging into a larger venule or vein at one of these sites. Transplantation of normal mammary ductal epithelium into mammary fat pads of nude mice served as transplantation control. Angiogenesis did not appear in the control ductal epithelial transplant 4-7 days post-transplantation.

Met-1 tumor microcirculation: angiogenesis started in the Met-1 tumor transplant 1-2 days post-transplantation. The tumor microvasculature could be conveniently divided into two separate microcirculations: a) the surface (external) microcirculation, and b) the intratumoral (internal) microcirculation (up to 250-350 μm inside the solid mammary tumors).

The external microcirculation originated from the surrounding subcutaneous and/or mammary fat pad vascular network(s). It consisted of varying numbers of supply arteries and normally one to two (at most three) drainage vein(s) which were detectable microscopically by 2-3 days. This external microcirculation became grossly visible 4-5 days post-transplantation. It started as small neovascular sprouts and developed into a complex network of vessels which spread to envelop the entire surface of the tumor mass by 10-23 days post-transplantation. The external vessels maintained relatively straight paths, and increased in size and organizational complexity with time.

The internal microcirculation could not be viewed or videotaped from outside the opaque solid tumor mass using conventional brightfield epi-illumination microscopy, but was clearly visible using the epi-fluorescence reverse illumination technique and specialized intravital microscopy (34-37).

Using this technology, internal angiogenic vessels could be detected and videotaped two days post-transplantation as small, at times incompletely formed, neovessels which lacked active blood flow. By four days post-transplantation, the angiogenic vessels increased in number and in diameter (increased from an average of 3 μm to 14 μm) (Fig. 1B) (Table II). Active blood flow was observed four days post-transplantation. The internal microcirculation went through a period of active growth and rapid development between 7 and 13 days post-transplantation. By 23 days, the internal vessels reached an average diameter of 84.6 μm (Table II). Their organizational pattern became increasingly complex; arterio-venous anastomoses were present, and the majority of the internal vessels exhibited tortuous paths (Fig. 1C and D).

The shape, complexity, organizational pattern and path of the internal microcirculation differed from the external surface microcirculation after seven days post-transplantation. When viewed under the intravital microscope, branches of the internal microcirculation were more complex and tortuous compared with the external vessels which exhibited relatively straight paths (Fig. 1E and F). The vessel distribution was dense close to the surface of the tumor. Microvascular distribution at the interior of the solid Met-1 tumor mass was heterogeneous; when approaching the center of the tumor, the microvessels were scattered, leaving some areas richly vascularized with clusters of tortuous vessels and some areas devoid of vessels.

Comparison of Met-1 and Db-7 microcirculation: in the first 2-6 days post-transplantation, the microcirculation in Met-1 and Db-7 was identical in both time-frame and morphometry. However, measurable differences began to appear 7-10 days post-transplantation. The diameters of the internal Met-1 microvessels were larger than Db-7 though the Db-7 tumors grew at a faster rate. The average diameter of Db-7 venules hovered close to the low range of normal for Met-1 in identical

time-frames [Met-1 average diameter (23 days) = 84.6±7.8 μm; Db-7 average diameter (23 days) = 68.1±5.4 μm; P<0.0001].

The relative abundance of internal vessels, the morphometric characteristics and the network organization were also different between Met-1 and Db-7 (Table II). The microcirculation inside Db-7 tumors was less complex in organization and path (tortuosity).

Necrotic areas inside the tumors could be identified by intravital microscopy as zones of increased opacity and without discrete cell outlines. These necrotic zones were totally devoid of functional vessels. More necrotic areas were observed in the interior of Db-7 tumors than Met-1 tumors. As predicted by these observations, scattered dead and fragmented vessels were found inside the Db-7 tumors, but not inside Met-1 tumors, at and beyond 23-days post-transplantation. The overall percent of the Db-7 tumor which was marginally or inadequately perfused (38) was significantly greater than Met-1 and normal control (Db-7 = 69.4%; Met-1 = 44.9%; subcutaneous tissue control = 5.6%; P<0.0001) (Table II).

In spite of the significant differences revealed in the study of the internal microcirculation between Met-1 and Db-7, no noticeable differences existed in their external microcirculation.

Microvascular pattern (vessel tortuosity). The external vessels were relatively straight in their paths (Fig. 1E) while the internal vessels were significantly more tortuous in Met-1 (Fig. 1D and F). These phenomena were expressed as the tortuosity index (TI) (shortest distance/actual distance between two reference points). The straightest path would be 1.0 and lower number indicate increasing tortuosity.

The TI of the external vessels of the Met-1 and Db-7 lines was not significantly different. However, the TI of the Met-1 internal vessels (average: 0.41) differed significantly (P<0.0001) from the TI of the Met-1 external vessels (average: 0.91) (Table II).

The internal vessels in Met-1 were significantly more tortuous than Db-7 (Figs. 1D, F and 2A, B). The TI of the internal vessels of Met-1 (average: 0.41) differed significantly (P<0.0001) from the TI of the Db-7 internal vessels (average: 0.78) (Table II).

Intratumoral microvessel density (MVD). Met-1 had more internal microvessels per unit area (surface area/region = 17.4±5.5; volume/region = 36.7±1.7) than Db-7 (surface area/region = 5.3±7.8; volume/region = 9.8±3.2). To correlate the three-dimensional *in vivo* quantitation of the internal microcirculation in this study with the two-dimensional analysis pioneered by Weidner *et al* (13-15), Gasparini *et al* (16), the intratumoral MVD was scored using histological sections of the Met-1 and Db-7 tumors. Intratumoral microvessels were identified by immunostaining (α-actin) of the MVD hot spots. Microvascular distribution inside solid tumors was heterogeneous. The MVD hot spot clusters were present in some areas and absent in other areas. However, whenever hot spots were located and scored, the MVD was high in Met-1 and low in Db-7. The high MVD in Met-1 (average: 20.2±9.7 microvessels per 200x field and 32.6±12.9 microvessels per 100x field) differed significantly (P<0.0001) from Db-7 (average: 7.6±3.8 microvessels per 200x field and 13.5±6.2 microvessels per 100x field).

Discussion

This report describes indices of microcirculation which distinguish between metastatic (Met-1) and low-metastatic (Db-7) tumor lines in a new transplantable mammary tumor model. The model is based on the serial transplantation of primary tumors from animals bearing the PyV-MT transgene promoted by the mouse mammary tumor virus long terminal repeat (31). The Met-1 line was derived from the wild-type PyV-MT transgene (31). The Db-7 was from animals bearing the PyV-MT with mutations at amino acids Y315 and Y322, which abrogate the interaction with phosphatidylinositol 3-kinase (32,33). The wild-type Met-1 line produced tumors that inevitably metastasized, consistent with the primary tumors from this transgenic line (31). Although the Db-7 developed mammary tumors, the Db-7 tumors metastasized at a much lower rate than Met-1 (8.8 vs. 100%, respectively).

This model system of mammary tumor metastasis provided an opportunity to compare the microvascular and cellular biology of two closely related mammary tumor cells with vastly different metastatic potential. The model may also be the basis for correlating the molecular biology and microcirculation with metastases. Some of the many common biological, clinical and microvascular correlates thought to be related to metastasis were studied in the course of this investigation.

The degree of differentiation is generally assumed to be related to the biological potential of the tumors. The Scarff, Bloom and Richardson (SBR) criteria are frequently used to evaluate the differentiation of human breast tumors (39). Like many grading systems, the lower scores indicate better differentiation. Surprisingly, when applied to the PyV-MT tumors, the Met-1 line scored lower in the SBR grading system in spite of its higher metastatic potential. The average SBR score for Met-1 was 4.7, while the low metastatic Db-7 line had an average score of 6.1. The metastatic potential of the PyV-MT transgenic mammary tumors was, thus, inversely related to the degree of cytological differentiation.

High growth rate has also been considered a poor prognostic feature in solid human tumors. In this study, the low metastatic Db-7 line had a higher growth rate than the metastatic Met-1 line. However, this difference might be misleading because the fast growing, low metastatic Db-7 line developed more necrotic sites than the metastatic Met-1 line. Therefore, the actual number of viable cells per unit volume could be lower than Met-1 [compare Figs. 1F and 2B]. The level of necrosis might be a controlling factor for metastasis in Db-7.

The relative metastatic potential of the Met-1 and the Db-7 tumors was directly related to the characteristics of the microcirculation. Indeed, this study has conclusively shown that the TI and MVD indices of the microcirculation in the metastatic Met-1 tumor line differed significantly (P<0.0001) from the low metastatic Db-7 line, confirming the usefulness of such indices. The extensive development of intratumoral microvessels in Met-1 could provide the primary tumors the routes for metastasis (13-16).

The previous experimental systems have been very useful for studying angiogenesis in initial stages of tumor growth in ectopic sites (3-6,22,23). However, the tumor transplants

could only be studied for the first 12-20 days using these systems (3-6,22,23). Since metastasis rarely develop within this short time-frame, the patterns of these early angiogenic vessels may not account for the metastases. Further, as the solid tumors grow they rapidly become opaque, obscuring the internal microcirculation and technically limiting studies to the external vessels. Since the MVD studies suggest that the intratumoral vessels are the most significant and only the external could be studied, the chamber type of experiment is clearly limited. Finally, many of these models involved ectopic site transplantation instead of the native orthotopic site of the mammary tumors. Some authors have suggested that ectopic transplantation could alter the biological potential of the transplanted tumor (29).

The combination of the experimental model system and experimental techniques described in this report has overcome many of the limitations described above. The biological limitations were addressed by developing a transplant system with known biological potential that could be studied as orthotopic as well as ectopic transplants. The technical limitations due to tumor opacity was overcome by using a novel system of specialized intravital microscopy and computer assisted image analysis with reverse epi-fluorescence illumination. The combination of approaches permits the observation and documentation of the intratumoral or internal microcirculation at depths of 250-350 μm inside tumors. The capture of the observed microcirculation on videotape and as digitized images permitted quantitative analysis of 25 different parameters (38).

Intravital microscopy with reverse epi-fluorescence illumination allowed *in vivo* analysis of living tumor tissues. Significant differences were demonstrated between the internal tumor microcirculation and the external microcirculation. The external vessels were straighter and more uniformly distributed over the surface of the tumor. Significantly, the external vessels of the two tumor lines were very similar and, thus, did not correlate with their metastatic potential. However, the internal microvessels in Met-1 were significantly denser, more deeply distributed, and more tortuous than those of the Db-7 ($P<0.0001$). Thus, quantitative analysis of the internal tumor microcirculation appeared to be more important than the external microcirculation for assessing metastatic potential.

The meandering paths of the microvessels could be measured and computed as a tortuosity index (TI) (shortest distance/actual distance traversed). It should be noted that TI for a straight path is unity (1.0). Increasing curvature is expressed as a decreasing proportion of unity. The TI of Met-1 internal microcirculation was at least two times lower than that of Db-7 indicating greater curvature. The TI proved to be a highly significant value that directly related to the biological potential (metastasis) of the tumor. The meandering path of a single microvessel observed in an *in vivo* three-dimensional setting (Fig. 1F), because of the plane of sectioning, might appear as many individual cross sections of the same vessel. Thus, the 'hot spots' used to calculate the MVD could represent the number of times a single vessel courses in and out of the tissue plane in a two-dimensional histological section. This interpretation suggests that the TI might be a more accurate mathematical reflection of the structure of tumor microcirculation. At the very least, the tortuosity index should be used as the standard indices in three-dimensional intravital studies of the microvasculature.

Other characteristics of the microvasculature, including vessel size and density (as measured by computer-assisted image analysis) also differed between Met-1 and Db-7 (Table II). Db-7 had smaller, fewer, and shorter vessels which had less surface area and less vessel volume per unit area, forming a more chaotic, or heterogeneous, microvascular bed. This heterogeneity was reflected in the differences in the percentage of area marginally perfused (Table II). Using the computer-assisted imaging technology developed previously to compute microvascular perfusion (38), the internal microcirculation of Db-7 was found to have significantly more marginally/inadequately perfused areas and much less adequately perfused areas ($P<0.0001$). Db-7 also had more fragmented, dead vessels and had necrotic zones on tissue sections. Thus, the microcirculation accurately reflected the degree of viability of the tumor.

A high MVD has been found to be an independent variable that correlated with poor prognosis in human breast cancer (13). The initial observations have been confirmed and extended in many studies (14-16). However, these retrospective clinical studies, to our knowledge, have never been verified experimentally. The microcirculation in samples of the mouse mammary tumors was estimated using standard techniques to count MVD. Met-1 tumors had consistently and significantly ($P<0.0001$) higher MVD than Db-7 tumors. Since the usual parameters such as growth rate and degree of differentiation of the tumors did not correlate with metastatic potential, the MVD proved to be the only histological variable studied which correlated with the biological potential of the two tumor lines. This is, to our knowledge, the first direct experimental verification of the relationship between internal tumor microcirculation development and mammary tumor metastasis.

In summary, we have described a controlled biological model of metastatic mammary tumors, a novel technique to study internal tumor microcirculation and introduced a new index (TI) for evaluating patterns of microcirculation. The experimental observations establish a physiological and quantitative confirmation of significant differences in the microcirculation of highly metastatic and low metastatic tumors. Since the technique permits the observation and quantitation of microvascular dynamics, we expect that the combination will provide valuable tools for the investigation of the functions of the microcirculation not previously available. Indeed, such quantitative analysis can lend itself to the discovery and description of more subtle alterations in the morphometry and function of the tumors. This technological advantage becomes crucial when studying internal vascular barriers to drug delivery (22) and in understanding and interpreting prognostic factors, such as TI and MVD, in human translation (13-16). The discovery of angiogenic growth factors and chemical modifiers of angiogenesis has given hope that neoplastic progress may be modified (19-21).

Acknowledgments

The research was supported in part by a grants from The W.G. Gilmore Foundation (San Francisco, CA) (A.T.W.C.), a Professional Development Award from the University of

California, Davis (A.T.W.C.), discretionary funds/gifts to the Biomedical Engineering Division in the Department of Medical Pathology (A.T.W.C.), a grant from BioSource, Inc. (Vacaville, CA) (R.D.C.), U.S. Department of the Army Grant DAMD17-96-1-6327 (R.D.C.), The Canadian Breast Initiative (W.J.M.), and U.S. Department of the Army Grant DAMD17-94-J-4300 (W.J.M.). W.J.M. is a Medical Research of Canada Scientist.

References

1. Jain RK: Determinants of tumor blood flow: a review. Cancer Res 48: 2641-2658, 1988.
2. Coman DR and Scheldon WF: The significance of hyperemia around tumor implants. Am J Pathol 22: 821-826, 1946.
3. Gullino PM and Grantham FH: The vascular space of growing tumors. Cancer Res 24: 1727-1732, 1964.
4. Grimbrone MA, Coltran RS, Leapman SB and Folkman J: Tumor growth and neovascularization: an experimental model using the rabbit cornea. J Natl Cancer Inst 52: 413-427, 1974.
5. Greenblatt M and Shubik P: Tumor angiogenesis: transfilter diffusion studies in the hamster by the transplant chamber technique. J Natl Cancer Inst 41: 111-124, 1968.
6. Cavallo T, Sade R, Folkman J and Coltran RS: Tumor angiogenesis: rapid induction of endothelial mitosis demonstrated by autoradiography. J Cell Biol 54: 408-420, 1972.
7. Folkman J and Coltran RS: Relation of vascular proliferation to tumor growth. Int Rev Exp Pathol 16: 207-248, 1976.
8. Folkman J: Tumor angiogenesis. Adv Cancer Res 43: 175-203, 1985.
9. Folkman J: How is blood vessel growth regulated in normal and neoplastic tissues? GHA Clowes memorial lecture award lecture. Cancer Res 46: 467-473, 1986.
10. Folkman J: Angiogenesis and breast cancer. J Clin Oncol 12: 441-443, 1994.
11. Warren BA: The vascular morphology of tumors. In: Tumor Blood Circulation. Petersen HI (ed). CRC Press, Boca Raton, FL, pp1-47, 1970.
12. Shubik P: Vascularization of tumors: a review. J Cancer Res Clin Oncol 103: 211-226, 1982.
13. Weidner N: Tumor angiogenesis: review of current applications in tumor prognostication. Semin Diagn Pathol 10: 302-313, 1993.
14. Weidner N, Semple JP, Welch WR and Folkman J: Tumor angiogenesis and metastasis - correlation in invasive breast carcinoma. N Engl J Med 324: 1-8, 1991.
15. Weidner N, Folkman J, Pozza F, Belvilacqua P, Allred E, Meli S and Gasparini G: Tumor angiogenesis: a new significant and independent prognostic indicator in early-stage breast carcinoma. J Natl Cancer Inst 84: 1875-1887, 1992.
16. Gasparini G, Weidner N, Bevilacqua P, Maluta S, Palma PD, Caffo O, Barbareschi M, Boracchi P, Marubini E and Pozza F: Tumor microvessel density, p53 expression, tumor size and peritumoral lymphatic vessel invasion are relevant prognostic markers in doe-negative breast carcinoma. J Clin Oncol 12: 454-466, 1994.
17. Folkman J: What is the evidence that tumors are angiogenic dependent? J Natl Cancer Inst 82: 4-6, 1990.
18. Folkman J and Klagsburn M: Angiogenesis factors. Science 235: 442-447, 1987.
19. Folkman J: Successful treatment of an angiogenic disease. N Engl J Med 320: 1211-1212, 1989.
20. Hockel M, Schlenger K, Doctrow S, Kissel T and Vaupel P: Therapeutic angiogenesis. Arch Surg 128: 423-429, 1993.
21. Battegay EJ: Angiogenesis: mechanistic insights, neovascular diseases, and therapeutic prospects. J Mol Med 73: 333-346, 1995.
22. Jain RK: Barriers to drug delivery in solid tumors. Sci Am 271: 58-65, 1994.
23. Yuan F, Salehi Y, Boucher Y, Vasthare US, Tuma RF and Jain RK: Vascular permeability and microcirculation of gliomas and mammary carcinomas transplanted in rat and mouse cranial windows. Cancer Res 54: 4564-4568, 1994.
24. Brem SS, Jensen HM and Guillino PM: Angiogenesis as a marker of preneoplastic lesions of the human breast. Cancer 41: 239-244, 1978.
25. Fogh J, Fogh JM and Orfeo T: One hundred and twenty-seven cultured human tumor cell lines producing tumors in nude mice. J Natl Cancer Inst 59: 221-225, 1977.
26. Giovanella BC and Fogh J: The nude mouse in cancer research. Adv Cancer Res 44: 69-120, 1985.
27. Ozello L and Sordat M: Behavior of tumors produced by transplantation of human mammary cell lines in athymic nude mice. Eur J Cancer 16: 553-559, 1980.
28. Sharkey FE, Fogh JM, Hajdu SI, Filtgerald PJ and Fogh J: Experience in surgical pathology with human growth in the nude mouse. In: The Nude Mouse in Experimental and Clinical Research. Fogh J and Giovanella BC (eds). Academic Press, New York, pp187-214, 1978.
29. Murthy MS, Scanlon EF, Jelachich ML, Klipstein S and Goldschmidt RA: Growth and metastasis of human breast cancers in athymic nude mice. Clin Exp Metastasis 13: 3-15, 1995.
30. Manzotti C, Audisio RA and Pratesi G: Importance of orthotopic implantation for human tumors as model systems: relevance to metastasis and invasion. Clin Exp Metastasis 11: 5-14, 1993.
31. Guy CT, Cardiff RD and Muller MJ: Induction of mammary tumors by expression of polyoma virus middle T oncogene: a transgenic mouse model for metastatic disease. Mol Cell Biol 12: 954-961, 1992.
32. Courtneidge SA and Hebner A: An 81 kDa protein complexed with middle T antigen and pp60c-Src: a possible phosphatidylinositol kinase. Cell 50: 1031-1037, 1987.
33. Whitman M, Caplan DR, Schaffhausen B, Cantley L and Roberts TM: Association of phosphatidylinositol kinase activity with polyoma middle T competent for transformation. Nature 315: 239-242, 1985.
34. Cheung ATW, Bry WI, Cox KL and Ahlfors CE: Reversal of microangiopathy in long-term diabetics after successful simultaneous pancreas-kidney transplants. Transplant Proc 25: 1310-1313, 1993.
35. Cheung ATW, Perez RV, Basadonna GP, Cox KL and Bry WI: Microangiopathy reversal in successful simultaneous pancreas-kidney transplantation. Transplant Proc 26: 493-495, 1994.
36. Cox KL and Cheung ATW: Bile flow rates and biliary microangiopathy quantitated by intravital microscopy. Biomat Med Cells Artif Org 17: 1-8, 1989.
37. Cox KL, Cheung ATW and Walsh EM: Intravital microscopy: a new *in vivo* technique for visualizing and quantifying effects of regulatory peptides on choledochoduodenal junction motility. Regul Pept 24: 1-14, 1989.
38. Chen PCY, Kovalcheck SW and Zweifach BW: Analysis of microvascular network in bulbar conjunctiva by image processing. Int J Microcirc Clin Exp 6: 245-255, 1987.
39. Le Doussal V, Tubiana-Hulin M, Friedman S, Hacene K, Spyratos F and Brunet M: Prognostic value of histologic grade nuclear components of Scarff-Bloom-Richardson (SBR). An improved score modification based on a multivariate analysis of 1262 invasive ductal breast carcinoma. Cancer 64: 1914-1921, 1989.

MOLECULAR AND CELLULAR BIOLOGY, Mar. 1992, p. 954–961
0270-7306/92/030954-08$02.00/0

Vol. 12, No. 3

Induction of Mammary Tumors by Expression of Polyomavirus Middle T Oncogene: A Transgenic Mouse Model for Metastatic Disease

CHANTALE T. GUY,[1] ROBERT D. CARDIFF,[2] AND WILLIAM J. MULLER[1]*

Institute for Molecular Biology and Biotechnology, McMaster University, 1280 Main Street West, Hamilton, Ontario, Canada L8S 4K1,[1] and Department of Pathology, School of Medicine, University of California at Davis, Davis, California 95616[2]

Received 23 September 1991/Accepted 2 December 1991

The effect of mammary gland-specific expression of the polyomavirus middle T antigen was examined by establishing lines of transgenic mice that carry the middle T oncogene under the transcriptional control of the mouse mammary tumor virus promoter/enhancer. By contrast to most transgenic strains carrying activated oncogenes, expression of polyomavirus middle T antigen resulted in the widespread transformation of the mammary epithelium and the rapid production of multifocal mammary adenocarcinomas. Interestingly, the majority of the tumor-bearing transgenic mice developed secondary metastatic tumors in the lung. Taken together, these results suggest that middle T antigen acts as a potent oncogene in the mammary epithelium and that cells that express it possess an enhanced metastatic potential.

The molecular basis underlying the ability of tumor cells to metastasize from the primary site of growth to other tissues is a major challenge in understanding oncogenesis. Metastasis likely involves a complex interaction between tumor cells, the extracellular matrix, adjacent stromal cells, and blood and/or lymphatic vessels. The products of several genes have been implicated as important determinants of the metastatic potential of a tumor cell. These include various proteases that are thought to play important roles in the turnover of basement membrane components such as collagen, glycoproteins, and proteoglycans. Evidence from a number of studies has suggested that the balance between expression of proteolytic enzymes and their inhibitors plays an important role in tumor invasion (22). In addition to the activation of proteases, metastasis may also involve alteration of cell surface determinants such as CD44 (14) or the function of the intracellular protein NM23 (20). Although the products of these genes contribute to the overall metastatic phenotype, the underlying causes responsible for their deregulation are still poorly understood. Ultimately, metastasis is thought to result from the aberrant expression of oncogenes or inhibition of their cognate regulators. For example, amplification and overexpression of a variety of oncogene products such as Neu/ErbB-2 and Int-2 have been inversely correlated with relapse and survival of affected cancer patients (21, 34).

While these clinical studies have provided important insights into oncogenesis, another useful model that has been used to study the role of oncogenes in tumor progression is the transgenic mouse. Transgenic mouse strains that express activated oncogenes in a variety of tissue types have been generated by a number of laboratories (16). Although many of these strains develop heritable malignancies, both the kinetics and apparent clonal nature of these tumors argue that additional genetic events are required for the cell to acquire the full malignant phenotype (16). By contrast to these observations, animals of one strain of transgenic mice uniformly expressing the activated *neu* tyrosine kinase under the transcriptional control of the mouse mammary tumor virus (MMTV) long terminal repeat (LTR) develop adenocarcinomas involving the entire mammary epithelium (26). Because these tumors arise synchronously and are polyclonal in origin, it was concluded that the expression of the activated *neu* protein was sufficient for transformation of the primary epithelial cell. These observations suggest that expression of activated *neu* tyrosine kinase at a certain threshold in the mammary epithelium can obviate the requirement for additional genetic alterations.

Another potent tyrosine kinase activity that has been implicated in the genesis of murine mammary tumors is that associated with the polyomavirus (PyV) middle T antigen. Infection of newborn or *nu/nu* mice with PyV results in the formation of a number of epithelial and mesenchymal tumor types of which mammary adenocarcinomas represent a significant proportion (4, 12, 37). Genetic analyses of PyV-mediated tumorigenesis has shown that a functional middle T antigen is required for tumor induction (17). The potent transforming activity of middle T antigen is dependent on its association with a number of cellular proteins. For example, there is compelling evidence that middle T specifically associates with and activates the tyrosine kinase activity of a number of c-*src* family members (c-*src*, c-*yes*, and *fyn*) (5, 7, 11, 18, 19). Furthermore, formation of this complex appears to be critical for middle T antigen to transform cells (9). In addition to association with tyrosine kinases, middle T antigen is also known to interact with the 85-kDa subunit of the phosphatidylinositol 3′-kinase (10, 40), and this association is also required for its transforming activity (37). More recently, stable complexes between protein phosphatase subunits A (regulatory) and C (catalytic) and middle T antigen have also been detected (27, 39). However, the role of such complexes in oncogenesis is unknown.

Given the ability of PyV middle T antigen to affect signal cell proliferation through a number of signal transduction pathways, we assessed its oncogenic potential in the mammary gland. To accomplish this, we directed the expression of the middle T antigen to the mammary epithelium by

* Corresponding author.

isolating transgenic mice carrying an MMTV-PyV middle T antigen fusion gene. Expression of middle T antigen in several independent transgenic strains resulted in the synchronous appearance of multifocal tumors involving all mammary glands. Because these tumors occurred early in mammary gland development and affected all transgenic animals, expression of the middle T oncogene appears to result in rapid conversion of the mammary epithelium to the transformed state. Interestingly, a majority of the middle T transgenic mice developed multiple metastases in the lung. The multifocal nature of these tumors and the high incidence of metastatic disease observed in these strains have important implications for understanding the molecular basis of tumor progression.

MATERIALS AND METHODS

DNA constructions. To derive the pMMTV MT construct, plasmid pmT165 (9) bearing the cDNA encoding the PyV middle T antigen (bounded by nucleotides 154 to 1560) (38) was cleaved with *Hin*dIII and *Eco*RI and inserted into corresponding *Hin*dIII and *Eco*RI sites of the PA-9-derived expression vector, pMMTV-SV40. The latter construct was established by first inserting the *Pst*I-to-*Bam*HI fragment bearing the simian virus 40 (SV40) small t splicing and polyadenylation signal from CDM8 (32) into the corresponding sites in plasmid Bluescript KS (Stratagene) and then cloning the MMTV LTR containing *Sal*I-to-*Hin*dIII fragment derived from plasmid pMMTV neuNT (26) into the corresponding sites of Bluescript KS. The β-casein riboprotection probe was obtained from J. Rosen and was cloned as a 205-bp *Pst*I fragment in plasmid pSP64 (Promega). The PyV middle T riboprotection probe pSP65mT (HA) was obtained from J. Hassell and contains a 203-bp *Hin*dIII-to-*Acc*I fragment of the PyV early region (PyV nucleotides 165 to 368) (35) inserted into the *Hin*dIII and *Acc*I sites of pSP65 (Promega). Finally, the internal control plasmid rpL 32 27.3.7, obtained from M. Shen, encodes an *Xho*II-to-*Dra*I fragment of the mouse ribosomal gene L32 inserted into the corresponding sites of plasmid Bluescript KS. All plasmids were isolated as described previously (33).

Generation and identification of transgenic mice. DNA was prepared for microinjection by digestion with 4 U each of *Sal*I and *Spe*I per μg for 1.5 h. The DNA was electrophoresed through a 1% agarose gel and purified as described previously (33). FVB female mice (Taconic Farms, Germantown, Pa.) were mated with FVB males the night before injection. After isolation of the fertilized one-cell mouse embryos, the pronuclei of these zygotes were injected with 0.5 to 1 pl of DNA solution (5 μg/ml). Following microinjection, viable eggs were washed once in M2 medium (29a) and transferred to the oviducts of pseudopregnant Swiss-Webster mice (Taconic Farms). To identify transgenic progeny, genomic DNA was extracted from a 1.5-cm tail clipping as described by Muller et al. (26). The nucleic acid pellet was resuspended in 100 μl of distilled water at an approximate DNA concentration of 1 μg/ml, and 15 μl of the DNA solution was digested with 30 U of *Bam*HI for 1.5 h. After gel electrophoresis and Southern blot transfer (36), the GeneScreen filters (Dupont) were hybridized with a PyV middle T cDNA probe radiolabelled with [α-^{32}P]dCTP by random priming (13).

Expression data. RNA was isolated from tissues by the procedure of Chirgwin et al. (8), using the CsCl sedimentation gradient modification. RNA yield was determined by UV adsorption at 260 nm after dissolving in sterile H_2O. RNA probes were made with either the Bluescript (Stratagene Inc., San Diego, Calif.) or pGEM vectors, and RNase protection assays were performed as described by Melton et al. (23), using 10 μg of total cellular RNA per assay.

In vitro kinase analyses. In vitro kinase assays were conducted as described by Aguzzi et al. (2). Tissue samples were ground to a fine powder by using a pestle and mortar cooled with liquid nitrogen and were lysed with 20 mM Tris (pH 8.0)–150 mM NaCl–1% Nonidet P-40–2.5 mM EDTA–1 mM sodium orthovanadate–10 mM NaF–1% aprotinin–10 mM leupeptin; 500 μg of total protein and 1 μg of rat polyclonal 3A1 (24) were incubated for 1 h at 4°C and then incubated with 30 μl of protein A-Sepharose beads for an additional hour. After five washes with TNE (50 mM Tris, 150 mM NaCl, 1% Nonidet P-40, 2 mM EDTA), the beads were resuspended in 25 μl of kinase buffer (20 mM morpholinepropanesulfonic acid [pH 7.0], 5 mM $MgCl_2$, 5 μCi of [γ-^{32}P]ATP) and incubated at 30°C for 20 min. Following a wash with 1 ml of TNE, the beads were resuspended in 50 μl of sample buffer (10 mM Tris [pH 6.8], 2% sodium dodecyl sulfate [SDS], 10% glycerol, 5% β-mercaptoethanol) and electrophoresed on 10% SDS-polyacrylamide gels.

Histological evaluation. Complete autopsies were performed as described by Muller et al. (26). Tissues were fixed in 4% paraformaldehyde, blocked in paraffin, sectioned at 5 μm, stained with hematoxylin and eosin, and examined as indicated in the legend to Fig. 3.

RESULTS

Generation of MMTV-PyV middle T antigen mice and tissue specificity of transgene expression. To derive transgenic mice expressing PyV middle T antigen in the mammary gland, a cDNA encoding PyV middle T antigen (38) was inserted into an MMTV LTR expression vector (Fig. 1A). The MMTV component was derived from plasmid PA9 (15), whereas the SV40 transcriptional processing signals at the 3′ end of the cDNA were obtained from plasmid CDM8 (32). To ensure that the MMTV/middle T antigen recombinant was biologically active, the transforming potential of the fusion gene was first assessed by transfection into Rat-1 cells. As expected, this construct was capable of transforming Rat-1 cells in the presence of supplemented glucocortocoids (data not shown). Before this plasmid was microinjected into one-cell mouse embryos, plasmid sequences were released by digestion with *Sal*I and *Spe*I (Fig. 1A). After injection of mouse zygotes, seven transgenic founder animals (MT#121, MT#196, MT#235, MT#634, MT#654, MT#668, and MT#670) were generated. With the exception of the two founder animals MT#235 and MT#196, both of which failed to transmit the transgene, the founders passed the transgene to their progeny in a Mendelian fashion.

To assess the tissue specificity of transgene expression, 10 μg of total RNA isolated from a variety of tissues was subjected to RNase protection analyses. As shown in Fig. 1B, the probe yields a 203-base protected fragment corresponding to the 5′ portion of the middle T cDNA. To ensure that approximately equal amounts of RNA from all organs were analyzed, an antisense probe from the mouse ribosomal protein L32-4A (kindly provided by M. Shen) was included in each hybridization reaction as an internal control. Representative results from these RNase protection analyses are shown for the MT#634 line in Fig. 1B. Both male and female carriers derived from this line developed extensive mammary tumors with early onset (Table 1). Female transgenic mice expressed high levels of the trans-

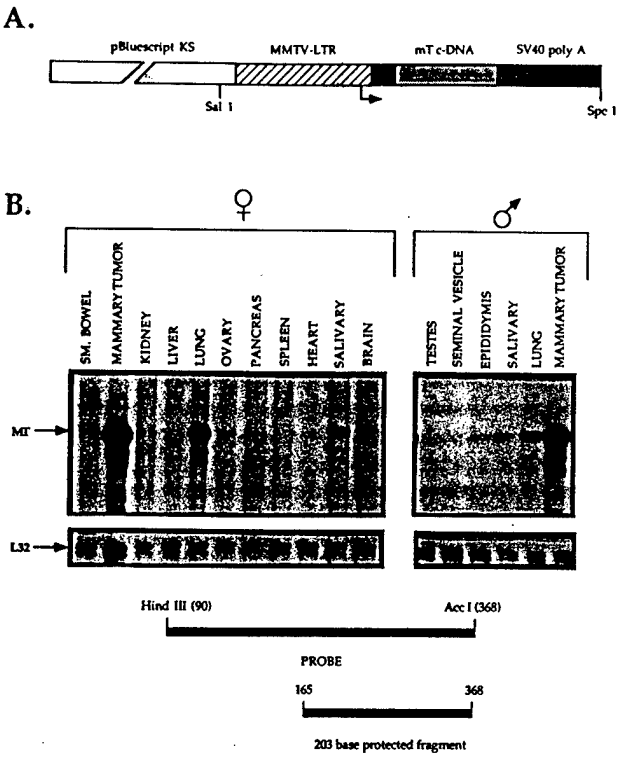

FIG. 1. Structure of transgene and tissue specificity of transgene expression. (A) Transgene structure. The unshaded region represents the sequences within the Bluescript vector backbone, the striped portion contains the MMTV LTR derived from plasmid pA9 (15), the filled region corresponds to an inert region derived from the original pA9 vector, the stippled region contains the cDNA encoding the PyV middle T antigen, and the adjacent cross-hatched region contains the transcriptional processing sequences derived from the SV40 early transcription unit. Relevant restriction sites and transcription start site (indicated by the arrow) are also shown. (B) RNA transcripts corresponding to the MMTV/middle T transgene in various organs of the MT#634 transgenic strain. Tissues were derived from a multiparous MT#634 female at 119 days of age (MT 5268) and an MT#634 male at 119 days of age (MT 2833). The antisense probe used in this RNase protection analysis (shown at the bottom) protects a 203-nucleotide fragment marked by MT and an arrow. Nucleotide numbers refer to the PyV early-region nucleotide sequence (35). Also shown is the RNase protection analysis with an antisense probe directed against the mouse L32 ribosomal gene. The L32 probe protects a 278-nucleotide fragment and is marked by L32 and an arrow. A lower band is also consistently observed in these RNase protections with the L32 probe.

gene product in the mammary tumors, with lower levels detected in the ovaries and salivary glands. Interestingly, in older (2 to 3 months) female transgenic animals, middle T transcripts were also detected in the lungs (Fig. 1B and 4B). This lung-specific expression was not observed in younger animals and is correlated with the appearance of multifocal lung metastases (see Fig. 4A). Male transgene carriers expressed high levels of the fusion gene in mammary tumors and lung metastases, whereas lower levels were detected in the salivary glands and epididymis.

The tissue specificity of transgene expression was also assessed for the remaining six transgenic animals of MMTV/middle T antigen mice by using the same RNase protection probe. As shown in Table 1, variable levels of transgene expression were noted in mammary glands of female transgenic mice derived from the MT#121, MT#668, MT#654, and MT#670 lines. Among the different female transgenic animals, considerable variation in both the amount and the temporal pattern of transgene expression was observed. For example, transgene transcripts were readily detected in the mammary glands derived from virgin female carriers of the MT#634 and MT#668 lines. By contrast, at least two pregnancies were required in order to detect similar levels of transgene expression in the MT#121, MT#654, and MT#670 strains (Table 1). As observed with the other transgenic strains, the appearance of these tumors was strictly correlated with the expression of the transgene. With the possible exception of the MT#196 transgenic founder, which developed mammary tumors, a seminal vesicle neoplasm, and hemanginomas, the lower amounts of middle T antigen RNA observed in the various tissues were not associated with any apparent growth disturbance.

To confirm that these transcripts encoded a functional middle T antigen, tissue extracts derived from the mammary glands of several of these transgenic lines were subjected to in vitro kinase assays using polyclonal antisera directed against middle T antigen. As a consequence of PyV middle T antigen's ability to associate with and activate a number of the *src* tyrosine kinases, the middle T protein becomes autophosphorylated on tyrosine residues in vitro (5, 7, 11, 18, 19). As illustrated in Fig. 2, a prominent 56-kDa phosphorylated band was observed in lanes incubated with the middle T-specific antisera. Because the band observed in the tumor extracts comigrated with middle T antigen derived from a Rat-1 cell line expressing middle T antigen, these observations suggest that the tumor extract possesses middle T-associated kinase activity. Incubation of the extracts with a nonspecific control antibody (mouse immunoglobulin G) resulted in the appearance of a background phosphorylated band that is present in all lanes. Consistent with the results of these in vitro kinase assays, Western immunoblot analyses also showed the presence of 56-kDa middle T protein in these tumors (data not shown). Together, these results indicate that the MMTV/middle T transgene in these strains associates with an active tyrosine kinase in the mammary epithelium.

Expression of the PyV middle T antigen in the mammary epithelium results in the generation of multifocal mammary tumors. Elevated expression of middle T antigen in the mammary glands of transgenic mice had dramatic consequences. In three of the five characterized transgenic lines, high levels of transgene expression were initially associated with the inability of female carriers to nurse their young. In addition, the MT#235 founder animal displayed an inability to lactate. In two of these transgenic lines (MT#634 and MT#668), this phenotype was apparent during the initial pregnancy, but the MT#121 strain demonstrated the nursing defect only after multiple pregnancies. Although there was some variation between these strains with respect to appearance of this phenotype, the inability to nurse was closely correlated with the onset of transgene expression (data not shown). By comparison with virgin female normal mammary tissue (Fig. 3A), whole-mount examination of virgin female mammary tissue from the MT#634 strain (3 weeks of age) revealed the presence of multiple mammary adenocarcinomas (Fig. 3B). These tumors were generally highly fibrotic, with dense connective tissue separating individual nests of tumor cells (Fig. 3C). By 5 weeks of age, all female carriers from the MT#634 (n = 35) and MT#668 (n = 4) lines had developed palpable mammary tumors (Table 1) that involved the entire mammary fat pad (Fig. 3C). The multifocal ap-

TABLE 1. Transgene expression and onset of tumors in MMTV/middle T mice[a]

Line	Sex[b]	Expression in:							Onset of tumor formation (days)	Tumor type(s)
		M.gl.	Sal	L	O	SV	T	Epi		
MT#121	F	+++	−	+	+				94 ± 18 (n = 20)	M.gl. adenocarcinoma
	M	−	−	−		−	−	−	NA	No tumor
MT#196 (founder)	M	+++	+	+		++	ND	ND	25 (n = 1)	Adenocarcinoma of M.gl. and seminal vesicles, hemangiomas
MT#235 (founder)	F	+++	−	−	+				70 (n = 1)	M.gl. adenocarcinoma
MT#634	F	+++	+	++	+				34 ± 6 (n = 35)	M.gl. adenocarcinoma
	M	+++	+	+		−	+	−	83 ± 20 (n = 20)	M.gl. adenocarcinoma
MT#654	F	+++	+	+	−				175 ± 68 (n = 2)	M.gl. adenocarcinoma
	M	−	−	−		−	−	−	NA	No tumor
MT#668	F	+++	++	+++	−				36 ± 2 (n = 3)	M.gl. adenocarcinoma
MT#670	F	+++	−	+	−				155 (n = 1)	M.gl. adenocarcinoma
	M	−	−	−		−	−	−	NA	No tumor

[a] RNase protection analysis was performed on 10 μg of total RNA isolated from a variety of organs in the MMTV/middle T strains as described in Materials and Methods. Relative levels of transgene expression are indicated by + (low), ++ (intermediate), and +++ (high). M.gl., mammary gland; Sal, salivary gland; L, lung; O, ovary; SV, seminal vesicle; T, testes; Epi, epididymis; NA, not applicable; ND, not determined; n, number of animals analyzed. All transgenic mice analyzed were tumor bearing.

[b] F, female; M, male.

pearance of mammary tumors in these strains was not dependent on pregnancy, because virgin female carriers displayed an identical tumor phenotype. The appearance of mammary tumors in the MT#121 line was closely correlated with the delayed onset of transgene expression, where 50% of female carriers at risk developed tumors by 94 days (Table 1). Despite the delayed kinetics of tumor formation, all multiparous MT#121 female carriers developed mammary tumors that eventually involved the entire mammary fat pad.

Male transgenic mice (n = 17) derived from the MT#634 strain also developed mammary adenocarcinomas with 100% penetrance, albeit with delayed onset (Table 1). The appearance of mammary tumors in male transgenic mice is consistent with results obtained with both male MMTV/v-Ha-*ras* and MMTV/activated c-*neu* transgenic mice (26, 33) and may result from expression of the oncogene in the male mammary epithelium prior to its normal regression. By contrast, male transgenic mice derived from the MT#121 strain did not develop mammary tumors, perhaps because of delayed onset of transgene expression. Both the rapid kinetics and the global nature of the tumor phenotype exhibited by these MMTV/middle T transgenic mouse strains suggest that expression of middle T antigen at appropriate levels can lead to transformation of the mammary epithelium.

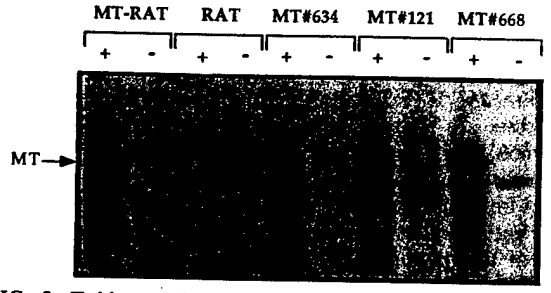

FIG. 2. Evidence that mammary tumors derived from the MMTV/middle T antigen strains possess middle T-associated tyrosine kinase activity. Shown are in vitro kinase activities of mammary tumor extracts derived from multiparous female MT#634 (MT 5524, 76 days old), MT#121 (MT 765, 154 days old), and MT#668 (MT 5532, 85 days old) carriers incubated with polyclonal rat antiserum directed against middle T antigen (+) or nonspecific antibody (−). Also included are a negative control with Rat-1 (RAT) fibroblasts and a positive control with middle T-transformed Rat-1 (MT-RAT) fibroblasts. The 56-kDa phosphorylated middle T antigen is indicated at the left (MT).

The middle T oncogene induces metastatic disease. As shown in Table 1, transgene expression was noted in the lung tissue of older individuals derived from the MT#634, MT#668, MT#654, MT#670, and MT#121 lines. Histological examination of lung tissue derived from MT#634, MT#668, MT#654, and MT#121 transgenic mice revealed the presence of multiple foci of metastatic mammary adenocarcinomas lodged in the lung parenchyma (Fig. 3D and 4A). By contrast to the primary mammary tumors, the pulmonary metastases contained little or no connective tissue separating nests of tumor cells (compare Fig. 3C and 3D). Because lung tissue was not obtained from MT#235 and MT#196 founder animals, it was not possible to assess whether middle T antigen expression observed in the lung was the result of metastatic disease. The extent of metastatic involvement in these lines was particularly remarkable with respect to both its degree and penetrance (Fig. 3D and 4A). For example, in the MT#634 strain, 94% of tumor-bearing females developed metastatic disease by 3 months of age. Male MT#634 tumor-bearing animals also developed metastatic disease, albeit with lower penetrance (80%). Similar proportions of the MT#121 (90%) and MT#668 (100%) tumor-bearing animals also developed metastatic disease during a 3-month observation period. Consistent with these observations, metastatic foci could be detected in either the lymphatic or the lung tissue after transplantation of the primary tumors from the tumor-bearing MMTV/middle T transgenic animals into the fat pads of normal syngeneic recipients (data not shown).

While these histological observations strongly suggested that the tumors in the lung were of mammary origin, further molecular analyses with mammary gland-specific probes were performed to establish this point. The metastatic nature of these lung tumors was confirmed by assessing whether these tumors were capable of expressing mammary differentiation markers such as β-casein. Using a probe directed to the 5′ end of the milk gene β-casein, RNase protection

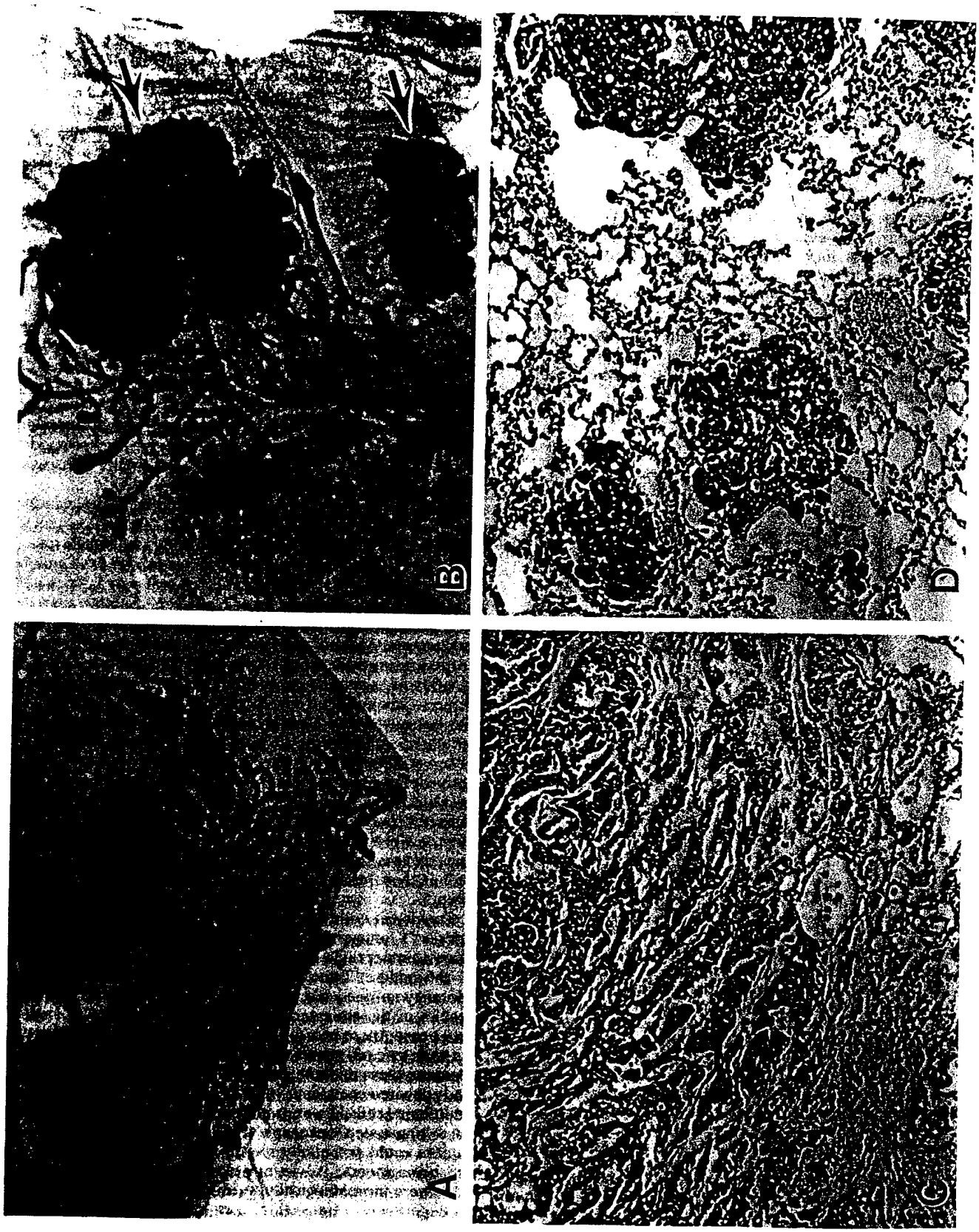
B
D
A
C

FIG. 3. Histopathology of MMTV/middle T transgenic mice. (A) Photomicrograph of a hematoxylin-stained whole mount of the mammary fat pad of a wild-type virgin mouse at 3 weeks of age showing normal growth and development. Magnification, ×16. (B) Photomicrograph of a hematoxylin-stained whole mount of the mammary fat pad of an MT#634 virgin transgenic female (MT 907) at 21 days of age. Compare with panel A. Note the irregular formation of side branches, enlarged terminal buds, and two large multilobular tumor masses (arrows). Magnification, ×16. (C) Photomicrograph of a sclerosing mammary adenocarcinoma from a middle T transgenic multiparous female mouse (MT#634 at 110 days). Note the dense connective tissue separating the attenuated cords of poorly differentiated mammary tumor cells. This pattern is typical of these transgenic mice. Magnification, ×87. (D) Photomicrograph of the lungs of the same mouse showing multiple metastases. Note that the tumor cells form well-defined acinar structures, with very little stroma separating the epithelium. Also note that the tumor cells are intra-alveolar rather than intravascular, indicating growth outside of the vessels. Magnification, ×87.

experiments were conducted on total RNA derived from both primary and lung tumors (Fig. 4B). Both the primary mammary tumor and lung metastases from the MT#634, MT#668, and MT#121 lines expressed moderate levels of β-casein transcripts. By contrast, RNA derived from normal lung tissue was completely devoid of any detectable β-casein mRNA. Taken together with the histological observations, these results demonstrate that expression of middle T antigen in the mammary epithelium leads to the development of metastatic disease.

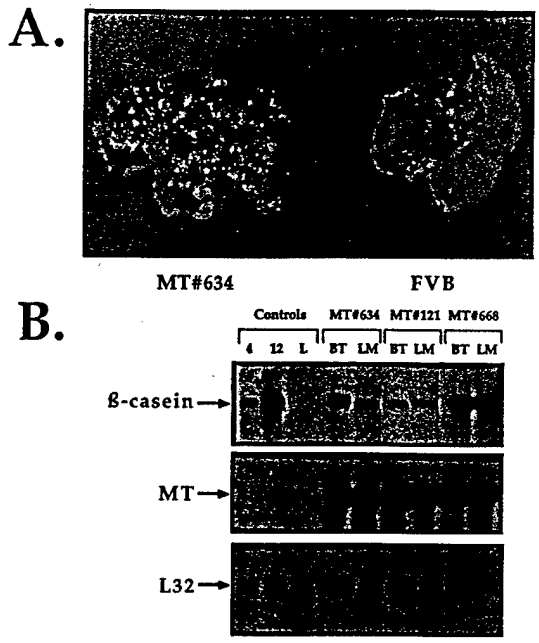

FIG. 4. Evidence that expression of the middle T oncogene results in metastatic mammary adenocarcinomas. (A) Lung tissue isolated from both MT#634 and FVB control animals. Note the extensive metastatic mammary tumors located throughout the lung tissue of the multiparous MT#634 female carrier (MT 5579) at 122 days of age. (B) RNase protection with control and transgenic tissues with probes directed to β-casein, middle T, and the L32 ribosomal internal control. The control tissues were isolated from the mammary glands of normal FVB mice and of 4-day (lane 4)- and 12-day (lane 12)-pregnant mice, as well as from normal lung tissue (lane L). Transgenic tissues derived from multiparous female MT#634 (MT 5579, 122 days), MT#121 (MT 5183, 130 days), and MT#668 (MT 5532, 85 days) carriers include primary breast tumors (lanes BT) and corresponding lung metastases (lanes LM). The 205-nucleotide protected fragment for β-casein, the 203-nucleotide protected fragment for middle T transcript (MT), and the 278-nucleotide protected fragment for the L32 ribosomal control are indicated by arrows.

DISCUSSION

Analysis of the transforming properties of the PyV middle T oncogene in the mammary epithelium provides important insight into the process of malignant progression. In four independent strains of MMTV/middle T transgenic mice, expression of the transgene ultimately resulted in the uniform morphological transformation of the mammary epithelium. Virgin female transgenic mice derived from the MT#634, MT#235 founder, and MT#668 strains developed multifocal adenocarcinomas as early as 3 weeks of age (Fig. 3B). Both the simultaneous occurrence of these tumors and their multifocal nature suggest that the expression of middle T oncogene is sufficient for mammary epithelial cell transformation.

The potent oncogenic potential of middle T antigen in the mammary gland is further supported by the results obtained with the MT#121 transgenic strain. In this particular transgenic line, mammary gland-specific expression of the middle T transgene was not detected until several pregnancies had occurred (data not shown). However, once transgene expression was observed, these animals developed multifocal mammary adenocarcinomas that eventually involved the entire mammary fat pad. Conceivably, the difference in the kinetics of transgene expression among the various transgenic strains could be influenced by the site of integration of the transgene. For example, variations in both the spatial and temporal patterns of transgene expression were also observed in transgenic mice bearing either the MMTV/activated *c-neu* transgene (26) or an elastase promoter-activated *ras* fusion gene (29). Moreover, the short latency between transgene expression and widespread morphological transformation of the mammary epithelium further argues that progression from a normal epithelial cell to a tumor cell in these mice requires few, if any, additional genetic events.

Consistent with this conclusion, previous studies of PyV middle T antigen in transgenic and chimeric mice have shown similar rapid tumor kinetics. For example, expression of the middle T oncogene under its own promoter or the Moloney murine leukemia virus promoter in transgenic mice results in disseminated endothelial tumors (3, 41). In the latter case, these hemaginomas resulted in embryonic lethality due to early onset of expression of middle T antigen. Because these endothelial tumors were polyclonal in nature and appeared coincident with the first appearance of yolk sac endothelial cells, it was proposed that middle T antigen acted as a single-step oncogene (41). However, because these tumors could potentially recruit normal endothelial cells to the hemaginoma, it was not clear whether all constituent cells were morphologically transformed (42). In another set of experiments, transgenic mice expressing the middle T oncogene in neuronal or epithelial tissues resulted in the formation of multiple neuroblastomas or carcinomas (2, 30).

However, because these transgenic animals exhibited preneoplastic lesions prior to the onset of tumor formation, additional genetic events were likely required.

The rapid tumor progression observed in the middle T oncogene transgenic mice contrasts with the observations made by a number of laboratories with transgenic mice bearing activated oncogenes. For example, multiple genetic events appear to be required for malignant progression in transgenic mice expressing oncogenes such as the SV40 large T antigen gene, c-*myc*, v-Ha-*ras*, or c-*fos* in a variety of different tissue types (1, 6, 31, 33). However, it has recently been reported that animals of one transgenic strain of mice carrying the activated *neu* gene under the transcriptional control of the MMTV LTR develop polyclonal mammary tumors without the need for a second event (26). It is interesting that both the activated *neu* and PyV middle T oncogenes are associated with constitutive tyrosine kinase activities that are refractory to normal cellular regulation. Determination of whether the powerful tissue-specific transforming activity exhibited by these oncogenes reflects the sensitivity of the mammary epithelial cell to a common tyrosine kinase signal transduction pathway awaits further analyses.

While the molecular basis for the potent transforming activity exhibited by the middle T oncogene is unclear, it is conceivable that deregulations of multiple signal transduction pathways through its association with the *src* family of tyrosine kinases, the phosphatidylinositol 3′-kinase, and phosphatase 2A individually contribute to the overall transformed phenotype. Indeed, PyV middle T antigen molecules impaired in their ability to deregulate either of these pathways display a pronounced reduction in the ability to transform cells in vitro or to induce tumors in animals (9, 37). Future experiments directed toward activating each of these signal transduction pathways individually in the mammary gland should allow this question to be addressed.

The unexpected finding that expression of the middle T antigen was closely associated with pulmonary metastases may provide important insight into the metastatic progression. By contrast to other MMTV/oncogene-bearing transgenic mice in which metastasis is a relatively rare occurrence (28), nearly all tumor-bearing MMTV/middle T transgenic carriers thus far analyzed developed metastatic disease. It is likely that these metastatic tumors originate from the primary mammary tumors because they still retain the capacity to express mammary markers such as β-casein. Consistent with this conclusion is the observation that transplantation of these primary mammary tumors into the fat pad of syngeneic recipients resulted in metastasis. The metastatic tumors were restricted to the lung and do not appear to seed other tissue sites. These metastatic foci appear to lodge in the vessels and grow by local expansion and invasion. The apparent specificity of these metastases to the lung may simply reflect the ability of the fine capillary beds of the lung to trap tumor emboli that have entered the bloodstream. Alternatively, the process of metastasis in this system may exhibit target specificity, perhaps mediated through the expression of ligand-specific cell adhesion molecules or the presence of a locally produced growth factor. Given the penetrance of metastatic disease observed in these lines, it is conceivable that middle T is activating cellular genes that are involved in metastatic progression. Because the PyV middle T tumors exhibit elevated proteolytic activity (unpublished observations), genes encoding various members of the protease family and their inhibitors may be potential downstream targets of the PyV middle T-associated tyrosine kinase. In fact, endothelial cells expressing PyV middle T antigen express high levels of urokinase plasminogen activator and low levels of its cognate inhibitor (PAI-1) (25). Determination of whether a similar proteolytic imbalance is responsible for the metastatic phenotype observed in the PyV middle T strains awaits further analysis.

ACKNOWLEDGMENTS

We thank Michael Shen, Lynn Matrisian, John Hassell, Joseph Bolen, Jeff Rosen, Dylan Edwards, and Philip Leder for providing the various nucleic acid probes and antibodies used in this study. In addition, we are grateful to Elisa Eiseman for providing protocols for performing in vitro kinase assays. We are also indebted to John Hassell, Malcolm Trimble, and Alison Cowie for critical reviews of the manuscript. We appreciate the excellent photographic support of Robert Munn.

This work was supported by research grants awarded by the National Cancer Institute of Canada and the Medical Research Council of Canada. This work was also partially supported by grant RO1-CAS4285 from the National Cancer Institute. W.J.M. is a recipient of a National Cancer Institute scientist award. C.G. was supported by a studentship provided by the Cancer Research Society.

REFERENCES

1. **Adams, J. M., A. W. Harris, C. A. Pinkert, L. M. Corcoran, W. S. Alexander, S. Cory, R. D. Palmiter, and R. L. Brinster.** 1985. The c-myc oncogene driven by immunoglobulin enhancers induces lymphoid malignancy in transgenic mice. Nature (London) **318**:533–538.
2. **Aguzzi, A., E. Wagner, R. L. Williams, and S. A. Courtneidge.** 1990. Sympathetic hyperplasia and neuroblastomas in transgenic mice expressing polyoma middle T antigen. New Biol. **2**:533–543.
3. **Bautch, V. L., S. Toda, J. A. Hassell, and D. Hanahan.** 1987. Endothelial cell tumors develop in transgenic mice carrying polyoma virus middle T oncogene. Cell **51**:529–538.
4. **Berribi, M., P. M. Martin, Y. Berthois, A. M. Bernard, and D. Blangy.** 1990. Estradiol dependence of the specific mammary tissue targeting of polyomavirus oncogenicity in nude mice. Oncogene **5**:505–509.
5. **Bolen, J. B., C. J. Theile, M. A. Israel, W. Yonemoto, L. A. Lipsich, and J. S. Brugge.** 1984. Enhancement of cellular src gene product-associated tyrosine kinase activity following polyomavirus infection and transformation. Cell **38**:767–777.
6. **Brinster, R., H. Y. Cheu, A. Messing, T. van Dyke, A. J. Levine, and R. D. Palmiter.** 1984. Transgenic mice harbouring SV40 T-antigen genes develop characteristic brain tumors. Cell **37**: 367–379.
7. **Cheng, S. H., R. Harvey, P. C. Espino, K. Semba, T. Yamanota, K. Toyoshima, and A. E. Smith.** 1988. Peptide antibodies to the human pp59 c-fyn is capable of complex formation with the middle-T antigen of polyomavirus. EMBO J. **7**:3845–3855.
8. **Chirgwin, J. M., A. E. Przybyla, R. J. MacDonald, and W. J. Rutter.** 1979. Isolation of biologically active ribonucleic acid from sources enriched in ribonuclease. Biochemistry **18**:5294–5299.
9. **Cook, D. N., and J. A. Hassell.** 1990. The amino terminus of polyomavirus middle T antigen is required for transformation. J. Virol. **64**:1879–1887.
10. **Courtneidge, S. A., and A. Hebner.** 1987. An 81 kDa protein complexed with middle T antigen and pp60 c-src: a possible phosphatidylinositol kinase. Cell **50**:1031–1037.
11. **Courtneidge, S. A., and A. E. Smith.** 1983. Polyoma virus transforming protein associates with the product of the c-src cellular gene. Nature (London) **303**:435–439.
12. **Dawe, C. J., R. Freund, G. Mandel, K. Ballmer-Hoffer, D. A. Talmage, and T. M. Benjamin.** 1987. Variations in polyoma virus genotype in relation to tumor induction in mice: characterization of wild type strains with widely differing tumor profiles. Am. J. Pathol. **127**:243–261.

13. **Feinberg, A. P., and B. Vogelstein.** 1983. A technique for radiolabeling DNA restriction endonuclease fragments to high specific activity. Anal. Biochem. **132**:6–13.
14. **Gunthert, U., M. Hofmann, W. Rudy, S. Reber, M. Zoller, I. Haussmann, S. Matzku, A. Wenzel, H. Ponta, and P. Herrlich.** 1991. A new variant of glycoprotein CD44 confers metastatic potential to rat carcinoma cells. Cell **65**:13–24.
15. **Huang, H. G., M. C. Ostrowski, D. Berard, and G. Hager.** 1981. Glucocorticoid regulation of the Ha-MuSV p21 gene conferred by sequences from mouse mammary tumor virus. Cell **27**:245–255.
16. **Hunter, T.** 1991. Cooperation between oncogenes. Cell **64**:249–270.
17. **Israel, M. A., H. W. Chan, S. A. Hourihan, W. P. Rowe, and M. A. Martin.** 1979. Biological activity of polyoma viral DNA in mice and hamsters. J. Virol. **29**:990–996.
18. **Kornbluth, S., M. Sudul, and H. Hanafusa.** 1986. Association of the polyomavirus middle T antigen with the c-yes protein. Nature (London) **325**:171–173.
19. **Kypta, R. M., A. Hemming, and S. A. Courtneidge.** 1988. Identification and characterization of p59 fyn (a src-like protein kinase) in normal and polyoma virus transformed cells. EMBO J. **7**:3837–3844.
20. **Leone, A., U. Flatow, C. Richter-King, M. A. Sandeen, M. K. Marguiles, L. Liotta, and P. Steeg.** 1991. Reduced tumor incidence, metastatic potential, and cytokine responsiveness of NM23-transfected melanoma cells. Cell **65**:25–35.
21. **Lidereau, R., R. Callahan, C. Dickson, G. Peters, C. Escot, and I. U. Ali.** 1988. Amplification of the INT-2 gene in primary human breast tumors. Oncogene Res. **2**:285–291.
22. **Liotta, L., P. Steeg, and W. G. Stelter-Stevenson.** 1991. Cancer metastasis and angiogenesis: an imbalance of positive and negative regulation. Cell **64**:327–336.
23. **Melton, D. A., P. A. Krieg, M. R. Rebagliati, T. Maniatis, K. Zinn, and M. R. Green.** 1984. Efficient in vitro synthesis of biologically active RNA and RNA hybridization probes from plasmids containing a bacteriophage SP6 promoter. Nucleic Acids Res. **12**:7035–7056.
24. **Mes, A. M., and J. A. Hassell.** 1982. Polyoma viral middle T-antigen is required for transformation. J. Virol. **42**:621–629.
25. **Montesano, R., M. S. Pepper, U. Mohle-Steinlein, W. Risau, E. F. Wagner, and L. Orci.** 1990. Increased proteolytic activity is responsible for the aberrant morphogenetic behaviour of endothelial cells expressing the middle T oncogene. Cell **62**:436–445.
26. **Muller, W. J., E. Sinn, P. K. Pattengale, R. Wallace, and P. Leder.** 1988. Single-step induction of mammary adenocarcinoma in transgenic mice bearing the activated c-neu oncogene. Cell **54**:105–115.
27. **Pallas, D. C., L. K. Shahrik, B. L. Martin, S. L. Jaspers, T. B. Miller, D. L. Brautigan, and T. M. Roberts.** 1990. Polyoma small and middle T antigens and SV40 small T antigen form stable complexes with protein phosphatase 2A. Cell **60**:167–172.
28. **Pattengale, P. K., T. A. Stewart, A. Leder, E. Sinn, W. Muller, I. Teplor, E. Schmidt, and P. Leder.** 1989. Animal models of human disease: pathology and molecular biology of spontaneous neoplasms occurring in transgenic mice carrying and expressing activated cellular oncogenes. Am. J. Pathol. **135**:39–61.
29. **Quiafe, C. J., C. A. Pinkert, D. M. Ornitz, R. D. Palmiter, and R. Brinster.** 1987. Pancreatic neoplasia induced by ras expression in acinar cells of transgenic mice. Cell **48**:1023–1034.
29a. **Quinn, P., C. Barros, and D. G. Whittingham.** 1982. Preservation of hamster oocytes to assay the fertilizing capacity of human spermatozoa. J. Reprod. Fertil. **66**:161–168.
30. **Rassoulzadegan, M., S. A. Courtneidge, R. Loubiere, P. El Baze, and F. Cuzin.** 1990. A variety of tumours induced by the middle T antigen of polyoma virus in a transgenic mouse family. Oncogene **5**:1507–1510.
31. **Ruther, U., C. Garber, D. Komitowski, R. Muller, and E. F. Wagner.** 1987. Deregulated c-fos expression interferes with normal bone development in transgenic mice. Nature (London) **325**:412–416.
32. **Seed, B., and A. Aruffo.** 1987. Molecular cloning of the CD2 antigen, the T cell erythrocyte receptor, by rapid immunoselection procedure. Proc. Natl. Acad. Sci. USA **84**:3365–3369.
33. **Sinn, E., W. Muller, P. Pattengale, I. Tepler, R. Wallace, and P. Leder.** 1987. Coexpression of MMTV/v-Ha-ras and MMTV/c-myc genes in transgenic mice: synergistic action of oncogenes in vivo. Cell **49**:465–475.
34. **Slamon, D. J., G. M. Clark, S. G. Wong, W. J. Levin, A. Ullrich, and W. L. McGuire.** 1987. Human breast cancer: correlation of relapse and survival with amplification of HER 2/neu oncogene. Science **235**:177–182.
35. **Soeda, E., J. R. Arrand, N. Smolar, J. E. Walsh, and B. E. Griffin.** 1980. Coding potential and regulatory signals of the polyomavirus genome. Nature (London) **283**:445–453.
36. **Southern, E. M.** 1975. Detection of specific sequences among DNA fragments separated by gel electrophoresis. J. Mol. Biol. **98**:503–517.
37. **Talmage, D. A., R. Freund, A. T. Young, J. Dahl, C. J. Dawe, and T. L. Benjamin.** 1989. Phosphorylation of middle T by pp60 c-src: a switch for binding of phosphatidylinositol 3-kinase and optimal tumorigenesis. Cell **59**:55–65.
38. **Treisman, R., U. Novak, J. Favaloro, and R. Kamen.** 1981. Transformation of rat cells by an altered polyoma virus genome expressing only the middle T protein. Nature (London) **292**:595–600.
39. **Walter, G., R. Ruediger, C. Slaughter, and M. Mumby.** 1990. Association of protein phosphatase 2A with polyoma virus medium tumor antigen. Proc. Natl. Acad. Sci. USA **78**:2521–2525.
40. **Whitman, M., D. R. Kaplan, B. Schaffhausen, L. Cantley, and T. M. Roberts.** 1985. Association of phosphatidylinositol kinase activity with polyoma middle T competent for transformation. Nature (London) **315**:239–242.
41. **Williams, R. L., S. A. Courtneidge, and E. F. Wagner.** 1988. Embryonic lethalities and endothelial tumors in chimeric mice expressing polyoma virus middle T oncogene. Cell **22**:121–131.
42. **Williams, R. L., W. Risau, H.-G. Zerwes, H. Drexler, A. Aguzzi, and E. F. Wagner.** 1989. Endothelioma cells expressing the polyoma middle T oncogene induce hemanginomas by host cell recruitment. Cell **57**:1053–1063.